FINAL REPORT

DESIGN OF MODEL OF A THERMOELECTRIC AIR CONDITIONING SYSTEM FOR SUBMARINES

E. W. FRANTTI

REPORT NO. 9161-01208-208 (I)

NEW PRODUCTS ENGINEERING DEPARTMENT
Westinghouse Electric Corporation

FINAL REPORT
DESIGN OF MODEL OF A THERMOELECTRIC AIR CONDITIONING SYSTEM FOR SUBMARINES

E. W. FRANTTI

NEW PRODUCTS LABORATORIES
WESTINGHOUSE ELECTRIC CORPORATION
PITTSBURGH, PENNSYLVANIA

CONTRACT NO. NOBS 77095

CHIEF, BUREAU OF SHIPS
DEPARTMENT OF NAVY
WASHINGTON 25, D. C.

FOREWORD

This report was the result of a contract initiated by the Chief, Bureau of Ships, Navy Department, Washington 25, D.C. The original research and development work upon which the report is based was accomplished by the New Products Laboratories, Westinghouse Electric Corporation of Pittsburgh, Pennsylvania, under Bureau of Ships Contract No. NOBS 77095. Mr. A. F. Phillips of Code 431 was the Project Officier. Mr. J. D. Meess of Westinghouse Electric Corporation was Supervisory Engineer in charge of work covered under the contract. Development started on 1 June 1959 and was completed on 1 May 1961.

Acknowledgement is made of the assistance provided by the personnel of Code 431 of the Bureau of Ships. Acknowledgement is also made of the invaluable assistance lent the author by Mr. R. S. Lackey and Mr. R. Chamberlin of Westinghouse Electric Corporation.

ABSTRACT

A thermoelectric heating and cooling module has been constructed for installation in a water to water air conditioning system aboard a submarine. This module has a cooling rating of 2550 BTU/hr. at a coefficient of performance of 0.75 and an operating current of 35 amperes dc. This rating was based on a 85°F sink water temperature and a chill water temperature of 55°F. The unit was designed to withstand submergence pressures and the corrosive effect of sea water in all water passages. It occupies a volume 1 ft. by 1 foot by 3 inches and was designed for ease in stacking into larger capacity units without additional space being required for coupling between units. It has a weight of 50 pounds.

Figure No. Page

TABLE OF CONTENTS

SUBMARINE THERMOELECTRIC AIR CONDITIONER

I. Introduction

The development of improved thermoelectric materials in recent years has enhanced their acceptability in many applications where heat pumping is required. Because they are static devices, their application in submarine air conditioning is especially attractive. During some periods of operation of a submarine, it is essential that the sound level be at a minimum. Present systems are inherently noisy and as it is not desirable to discontinue air conditioning at any time, a need has arisen for a quiet system of air conditioning. Thermoelectric heat pumps appear to be ideal for this application. For this reason, the Navy had initiated this development as a step in a program to obtain shipboard systems and components utilizing thermoelectric materials. This development was intended to determine performance characteristics of available thermoelectric materials, to evaluate and solve problems relative to fabrication and heat transfer in a practical device, to evaluate practicality for submarine application, and determine in which areas major efforts should be directed.

With these purposes in mind, the development was to lead to the design and construction of a model submarine air conditioning and refrigeration system. This model was to utilize sea water as a heat sink and fresh water as the chilled medium by which cooling was to be dispersed throughout the ship. In other words, this development was specifically directed toward the development of a water to water system in which heat is pumped from one water loop to another.

II. Theory

The basis of the thermoelectric effect is that conduction electrons in different materials have different average energy levels. In a semiconductor the electrons in the conduction band have a higher average energy than the electrons in the conduction band of a metal. Thus, in the junction of a suitable semiconductor and a metal an electron current, due to an applied field, flowing from the metal to the semiconductor, will transfer thermal energy from the metal to the semiconductor. On the other end of the semiconductor where the electron flow leaves to enter a metal again the thermal energy will be released to the metal. This is a greatly simplified explanation of the thermoelectric or Peltier effect. There are many other factors which influence the operation of a thermoelectric junction. The rate of heat pumped through the material per unit of current flowing is called the Peltier coefficient, π.

Rate of heat flow, $Q = \pi I$

If a materials is heated on one end there will be an increase in the concentration and velocity of electrons at the hot end, which will result in the diffusion of electrons toward the cold end. The cold end then becomes negatively

charged with respect to the hot end. This potential difference caused by the difference in temperatures between the ends of the material is called the Seebeck effect. The Seebeck coefficient (α) or thermoelectric power of a material is defined as the ratio of the potential difference to the temperature difference.

$$\alpha = \frac{\Delta E}{\Delta T}$$

The Peltier coefficient (π) is related to the Seebeck coefficient (α) by,

$$\pi = \int_{o}^{T} \alpha \, d \, T$$

where T is the absolute temperature. In metals the value of α is of the order of microvolts per degree centigrade while in semiconductors, it is of the order of millivolts per degree centigrade.

So far, we have considered only the transfer of heat by electron flow. A thermoelectric material of this type in which the major current carriers are electrons is classed as an N-type material. Although a cooling system can be made using only a metal such as copper and an N-type semiconductor, this would give very poor performance as shown in Figure 1.

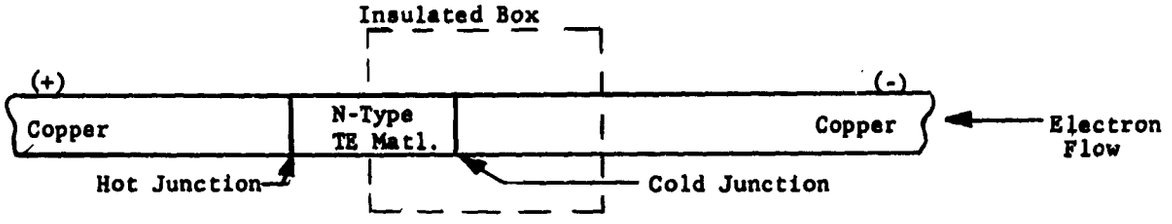

FIGURE 1

If the cold junction were enclosed in an insulated box, as is usually desirable, it can be seen that heat would leak into the box through the copper. There are, however, some materials which are classed as P-type materials in which the major current carriers are "holes". Basically, a hole is a vacancy in the valence band of a semiconductor caused by an electron moving into the conduction band. These holes behave in the same way as free electrons possessing a positive charge. These materials when heated at one end will develop an electric field opposite to that of the N-type material, and will transfer heat similarly to electrons but in the opposite direction. Thus, a practical heat pumping device or thermoelectric couple can now be constructed as in Figure 2.

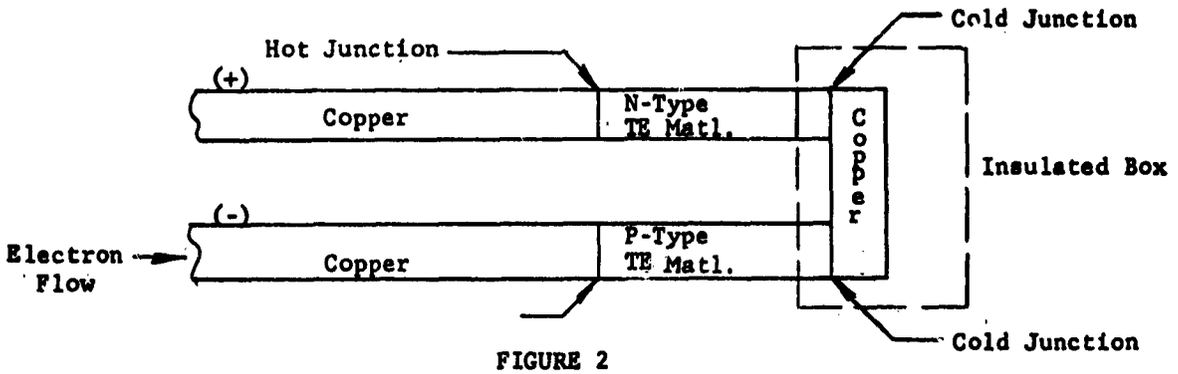

FIGURE 2

There is now no heat leakage into the insulated box through the electrical current conductors, as both the positive and negative electrical connections are made on the hot junctions of the thermoelectric couple which are outside the box. There is no theoretical necessity for the copper shown in the box connecting the N and P type material together. The couple would perform as well if the N and P type material were butted end to end. However, for practical purposes, they are joined with a copper strap for convenience and to provide a relatively large surface area through which the heat from within the box can enter the junction.

Thus far, we have considered only the Peltier coefficient of thermoelectric material and know that the heat pumping or cooling rate is proportional to the electric current flowing through the material. Thus, the more current that is passed through the material, the more heat can be pumped. This is basically true except that there are other major factors which enter in and limit the heat pumping rate. The first of these is the electrical resistance of any material to current flow. This resistance to current flow produces the so called Joulean heat or more conventionally the I^2R loss in the material. As can be seen, this heat is proportional to the square of the current and the resistivity of the material. However, since it is uniformly distributed throughout the material only 1/2 of it is considered as opposing the Peltier heat flow. The second effect is that caused by heat conduction through the material itself from the hot junction to the cold junction. This heat leakage directly opposes the Peltier heat flow and is proportional to the temperature difference between the hot and cold junction and the thermal conductivity of the material. The rate of heat pumping of a thermoelectric material then can be expressed by the equation,

$$Q = \pi I - 1/2\ I^2 \rho \frac{L}{A} - K \frac{A}{L} (T_h - T_c)$$

where π = Peltier coefficient

I = Electric current

ρ = Resistivity of thermoelectric material

L = Length of thermoelectric material

A = Cross-section area of thermoelectric material

K = Thermal conductivity of thermoelectric material

T_h = Temperature of hot junction

T_c = Temperature of cold junction

From this basic equation and the equation relating the Seebeck and Peltier coefficients it can be seen that thermoelectric materials should have the following characteristics.

1. A large thermoelectric power (α)
2. A low electrical resistivity (ρ)
3. A low thermal conductivity (K)

These three properties can be combined into a figure of merit which characterizes the thermoelectric ability of a material.

$$Z = \frac{\alpha^2}{\rho K}$$

It is the success in the optimization of this figure of merit which has brought about the recent upsurge in thermoelectric device development. Figures of merit of $3.0 \times 10^{-3}/C^\circ$ and higher have been reported by various investigators. For the usual materials the thermoelectric power ranges around 200 microvolts per degree centigrade, the resistivity around 1 milliohm-cm., and the thermal conductivity around 0.02 watts/cm C°. This figure of merit is applicable to both N and P type material separately, and if both the N and P type material used are assumed to have identical properties it will also be applicable for a couple. This assumption makes possible a simple and convenient method of experimentally determining the figure of merit of a couple. By differentiating the basic heat pumping equation with respect to the current,

$$Q = \pi I - 1/2\ I^2 \rho \frac{L}{A} - K \frac{A}{L} (T_h - T_c)$$

$$\frac{dQ}{dI} = \pi - I \rho \frac{L}{A}$$

and equating it to zero, the current for maximum heat pumping can be obtained.

$$I_{Qmax} = \frac{\pi}{\rho}\frac{A}{L}$$

Substituting this current into the basic heat pumping equation and setting Q, the heat pumping rate, to zero the maximum temperature differential between the hot and cold junctions is found in terms of the material parameters.

$$0 = \pi \left(\frac{\pi A}{\rho L}\right) - 1/2 \left(\frac{\pi A}{\rho L}\right)^2 \frac{\rho L}{A} - \frac{K A}{L} (T_h - T_c)$$

$$0 = \frac{\pi^2 A}{\rho L} - 1/2 \frac{\pi^2 A}{\rho L} - \frac{K A}{L} (T_h - T_c)$$

$$(T_h - T_c) = 1/2 \frac{\pi^2 A}{\rho L} \times \frac{L}{K A} = 1/2 \frac{\pi^2}{\rho K}$$

Substituting for the Peltier coefficient its equivalent in terms of thermoelectric power gives the figure of merit in terms of temperatures which are easily measured.

$$\pi = \int_0^{T_c} \alpha \, d T \doteq \alpha T_c$$

$$\frac{2(T_h - T_c)}{T_c^2} = \frac{\alpha^2}{\rho K} = Z$$

A simple device as shown in Figure 3 can be made to determine the figure of merit based on this equation. The hot junctions are maintained at some specific temperature while the cold junction is allowed to reach its lowest temperature with maximum Q current supplied under adiabatic conditions, that is, with no heat entering the cold junction.

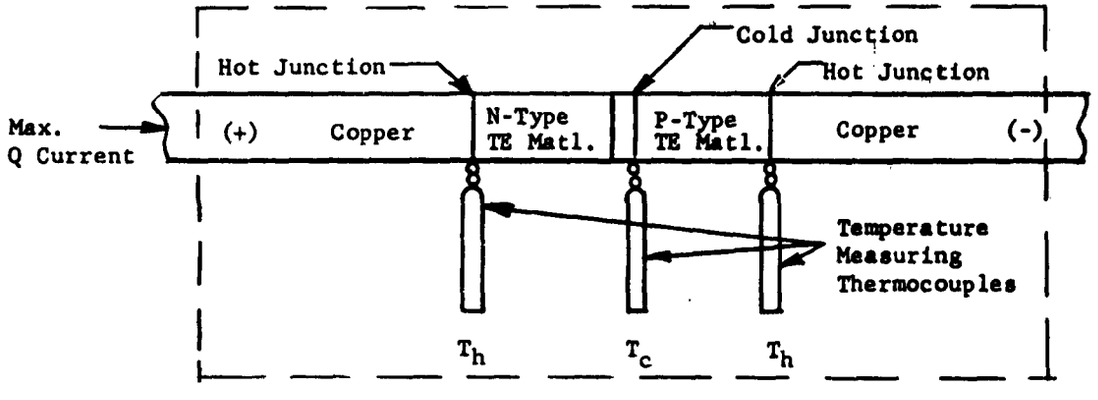

FIGURE 3

The coefficient of performance of a thermoelectric cooling system is expressed as the ratio of the heat removed in a unit time to the electric power consumed.

$$C.O.P. = \frac{Qc}{W}$$

The power consumed consists of the I^2R loss plus the power required to overcome the thermal emf generated due to the temperature differential across the couple.

$$W = I^2R + \alpha (T_h - T_c) I$$

The C.O.P. can then be written as

$$C.O.P. = \frac{\alpha I T_c - 1/2 \frac{I^2 \rho L}{A} - \frac{K A}{L} (T_h - T_c)}{I^2R + \alpha (T_h - T_c) I}$$

This expression can be differentiated with respect to the current, I, and equated to zero to obtain the maximum C.O.P. current and the corresponding maximum C.O.P. which can be written in the form,

$$\text{Max. C.O.P.} = \frac{T_c}{T_h - T_c} \times \frac{1 + 1/2 Z (T_h - T_c) - \frac{T_h}{T_c}}{1 + 1/2 Z (Th - T_c) + 1}$$

This expression shows that the performance of a thermoelectric cooling device improves with increase in value of the figure of merit and approaches the ideal efficiency of the Carnot cycle.

$$\eta_c = \frac{T_c}{T_h - T_c}$$

In general, thermoelectric cooling systems are operated between the limits of maximum heat pumping rate and maximum coefficient of performance. Since these two conditions cannot be satisfied simultaneously, a balance must be decided upon. Figure 4 graphically depicts the operation of a typical thermoelectric couple. Once the operating point has been decided upon, the heat exchangers for the hot and cold junctions are then designed to remove or absorb the calculated amount of heat. If the cooling unit is constructed in this manner, the performance of the unit will not follow exactly the curves of Figure 4 with increasing current, but will reach its maximum Qc at the design point and then fall off in total heat pumping rate as well as in coefficient of performance. This is because the hot side heat exchanger increases rapidly in temperature with increase in current above the design point.

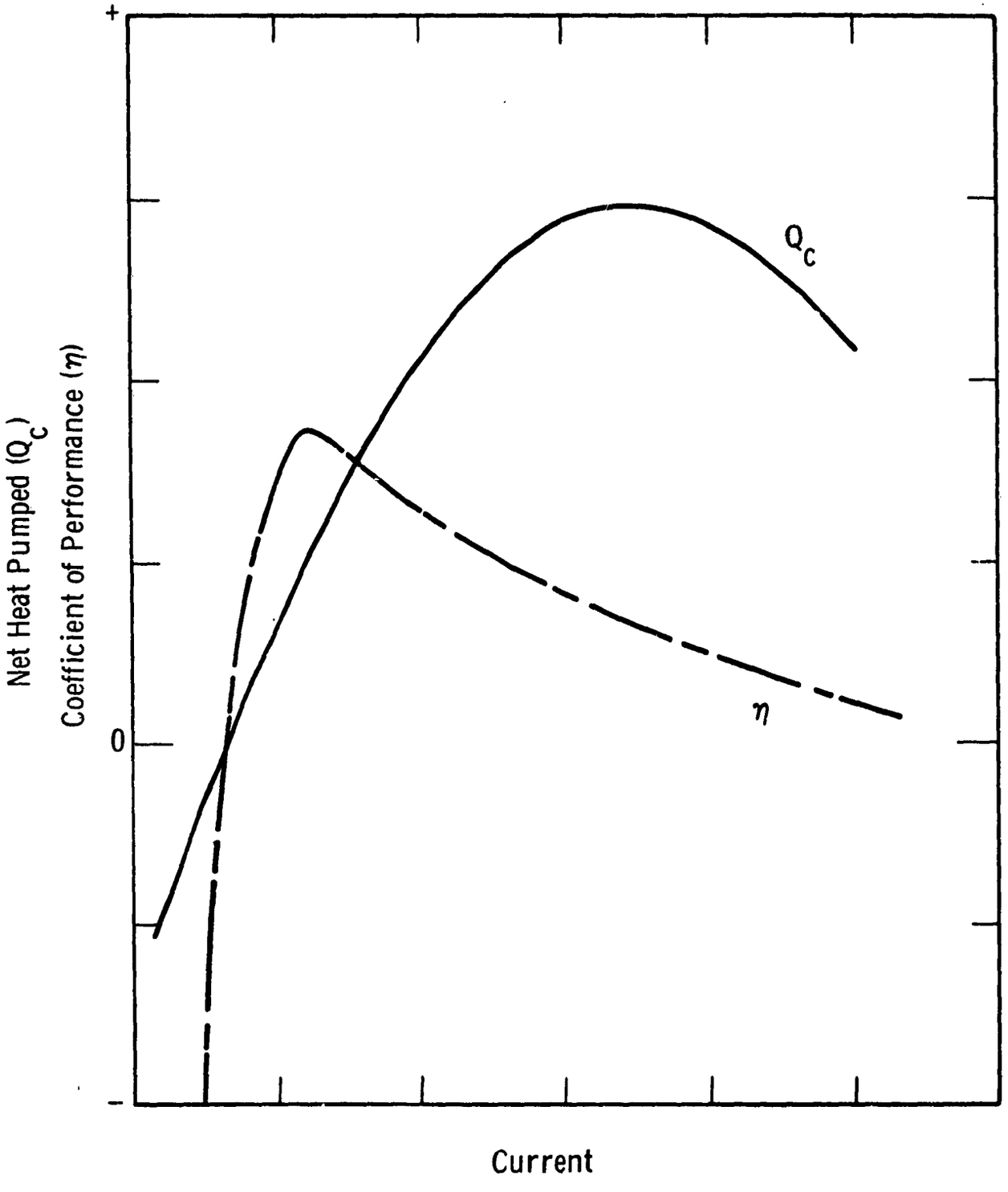

Fig. 4 —Heat Pumping Characteristics of a Typical Thermoelectric Couple

Typical construction of a thermoelectric couple is shown in Figure 5.

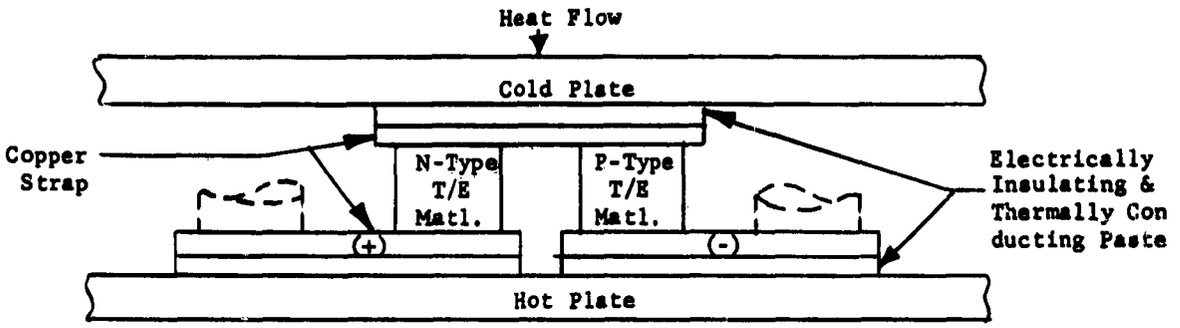

FIGURE 5

As many couples are necessary to produce the required heat pumping are connected in series between the hot and cold plate. The electrically insulating but thermally conducting paste is a mixture of aluminum oxide and silicon grease. It is used to prevent the couples from shorting one to the other and to provide good thermal contact to the hot and cold plates. The hot and cold plates which are of aluminum are also "hard-coated" to aid in the prevention of shorts. The couples are constructed by first soldering the elements to the hot side copper straps and then fastening these straps, with elements attached, to the hot plate. The copper straps which make up the cold junctions are then all soldered at one time to the elements in a jig, so that the cold junction straps will all lie in one plane. The cold plate is then placed in thermal contact with the cold junction straps and fastened to the hot plate to make a mechanically rigid unit. This process can be reversed in that the copper straps can be first fastened to the cold plate and the jig soldering accomplished on the hot junctions. Although in Figure 5, the cold and hot plates are shown simply as plates, in the usual application they are heat exchangers which absorb heat on the cold side and dissipate heat on the hot side.

III. Module #1 Design

Consistent with the requirements as set forth by the Bureau of Ships, the decision was made to construct a small subsection or module several of which tied together would supply the required 1 ton heat pumping capacity. This first module was considered to be a prototype of the units to follow. Our approach to the problem was to construct a sandwich type of unit in which one chill water heat exchanger would be sandwiched in between two sink water heat exchangers.

Separating the heat exchangers one from another would be the thermoelectric material which would be arranged to extract heat from the center or chill water heat exchanger and dissipate it in the outer or sink water heat exchanger. The heat exchangers were constructed of coiled aluminum tubing brazed to a flat

aluminum plate as shown in Figure 6 and 7. The aluminum plate surface serving as the thermal contact area between the thermoelectric material and the heat exchanger. The chill heat exchanger was constructed of two aluminum plates with the tubing brazed in between while the two sink heat exchangers consisted of one aluminum plate with the tubing brazed to the outside. This type of construction was used as it was felt the tubing could be readily made to withstand submergence pressure in future designs.

As a starting point for the design, an output rating goal of 1000 BTU/hr at maximum coefficient of performance was chosen. The calculations on which the design was based are shown in Appendix I. In Figure 8 is shown the arrangement of the thermoelectric pellets on the chill water heat exchanger. A 196 thermoelectric couples of 0.420 inch diameter and 0.25 inch long were used per module with 98 couples on each side of the chill water heat exchanger. As shown in Figure 8, the pellets were first soldered to copper straps 1-1/2 inches x 3/4 inch x 1/16 inch which were fastened to the heat exchanger by nylong screws. Electrical insulation between the straps and the heat exchanger was provided by anodizing the heat exchanger surface and by a thin layer of aluminum oxide and silicon oil paste. This paste also assured good thermal contact between the plate and the heat exchanger. The nylon screws were used to prevent electrical contact between strap and heat exchanger. The next step in the assembly of the unit was the soldering of the hot junction straps to the thermoelectric material. This was done using a flat aluminum plate or jig on which the copper straps were held in correct position by steel pins which protruded through the jig. These pins were loose fitting so that they would fall out when the jig was lifted. The procedure then was to place the jig with straps and pins in place on a hot plate which could be raised to soldering temperature. The chill heat exchanger with thermoelectric pellets attached was then lowered onto the jig in correct position and allowed to solder. The jig was then raised and all pins removed. After cooling the assembly was as shown in Figure 9. The other side of the chill heat exchanger was then soldered. To finish the assembly, the two sink heat exchangers were bolted on with through bolts so that the whole assembly was squeezed together. Here again the heat exchanger surfaces were anodized and coated with the aluminum oxide silicon oil paste. The thermoelectric couples on either side were connected in electrical series, however, they could have been connected in parallel as the couples would function the same as long as the current through each pellet was identical. The water paths through the sink heat exchangers were also connected in series for convenience. The figure of merit of the thermoelectric material used averaged 2.28×10^{-3} 1/C° as measured using the ΔT method as previously described. To prevent undue heat leakage between heat exchangers, the space between pellets was filled with silica aerojel. Later on the aerojel was replaced with polyurethane foam.

Included in the contract requirements was the construction of a two cubic foot thermoelectric freezer using the chill water as a heat sink. The thermoelectric assembly was similar to the module construction except for two major changes. The same size thermoelectric material was used, but the pellets were soldered unto copper pegs. This was done to decrease the heat leakage between the hot and cold junctions. The sink heat exchanger construction was identical with the module sink heat exchangers, however the chill heat exchanger was constructed of aluminum fins brazed to an

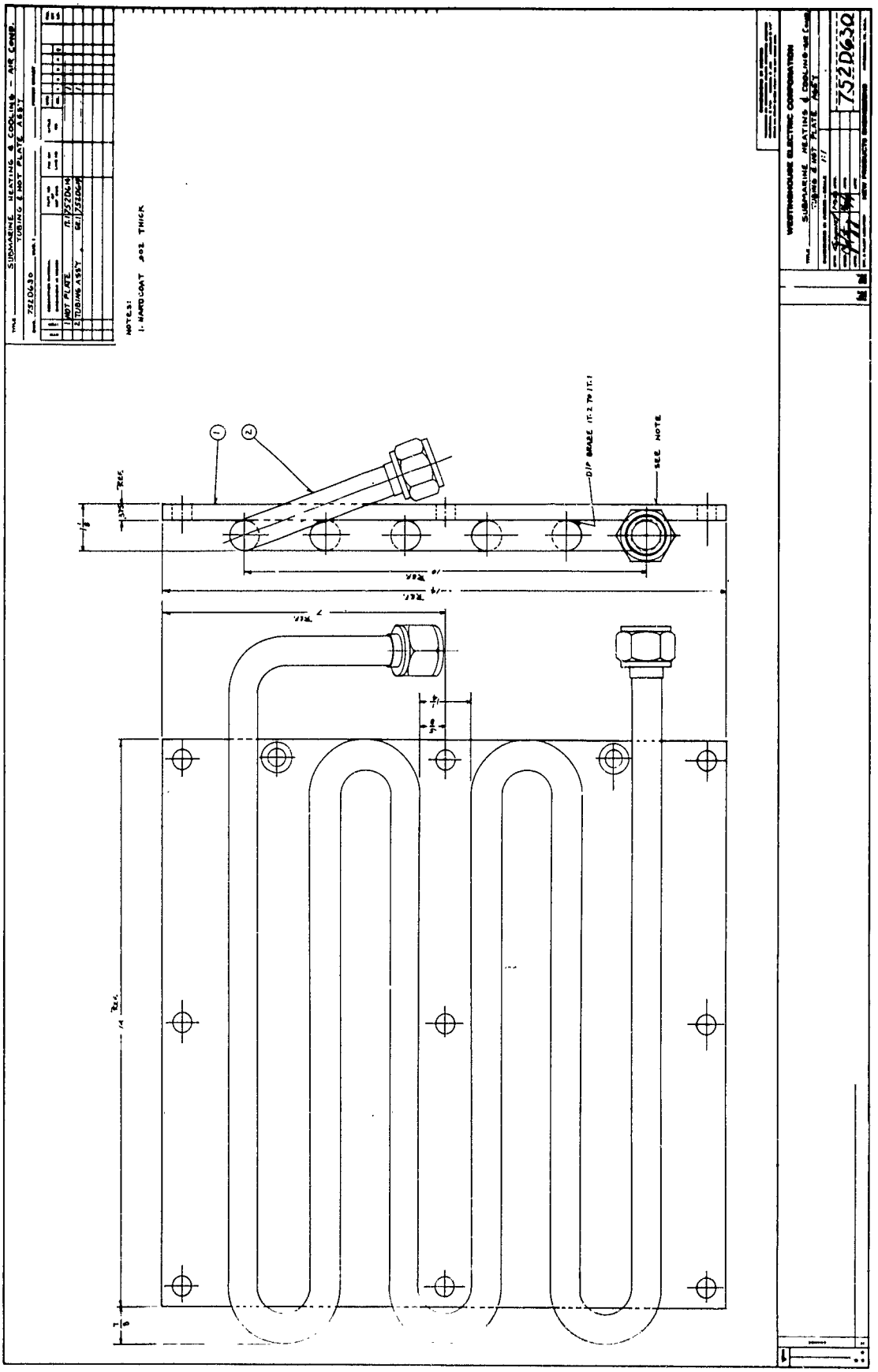

Figure 6 Module 1 Sink Water Heat Exchanger Drawing

N.P.M.- 533

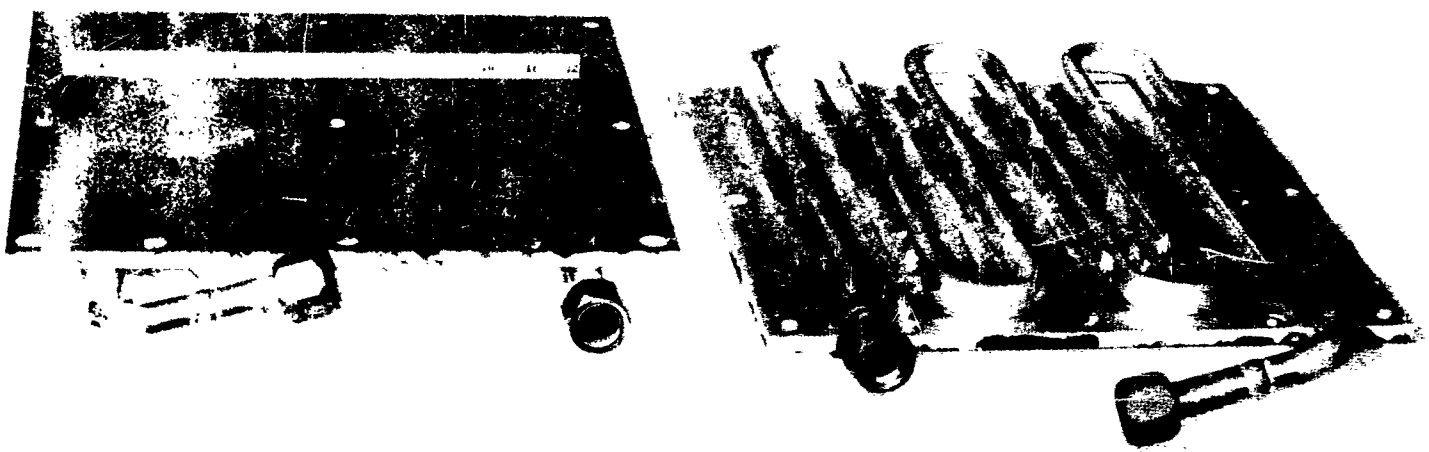

Figure 7 Module 1 Sink Water Heat Exchanger Photograph

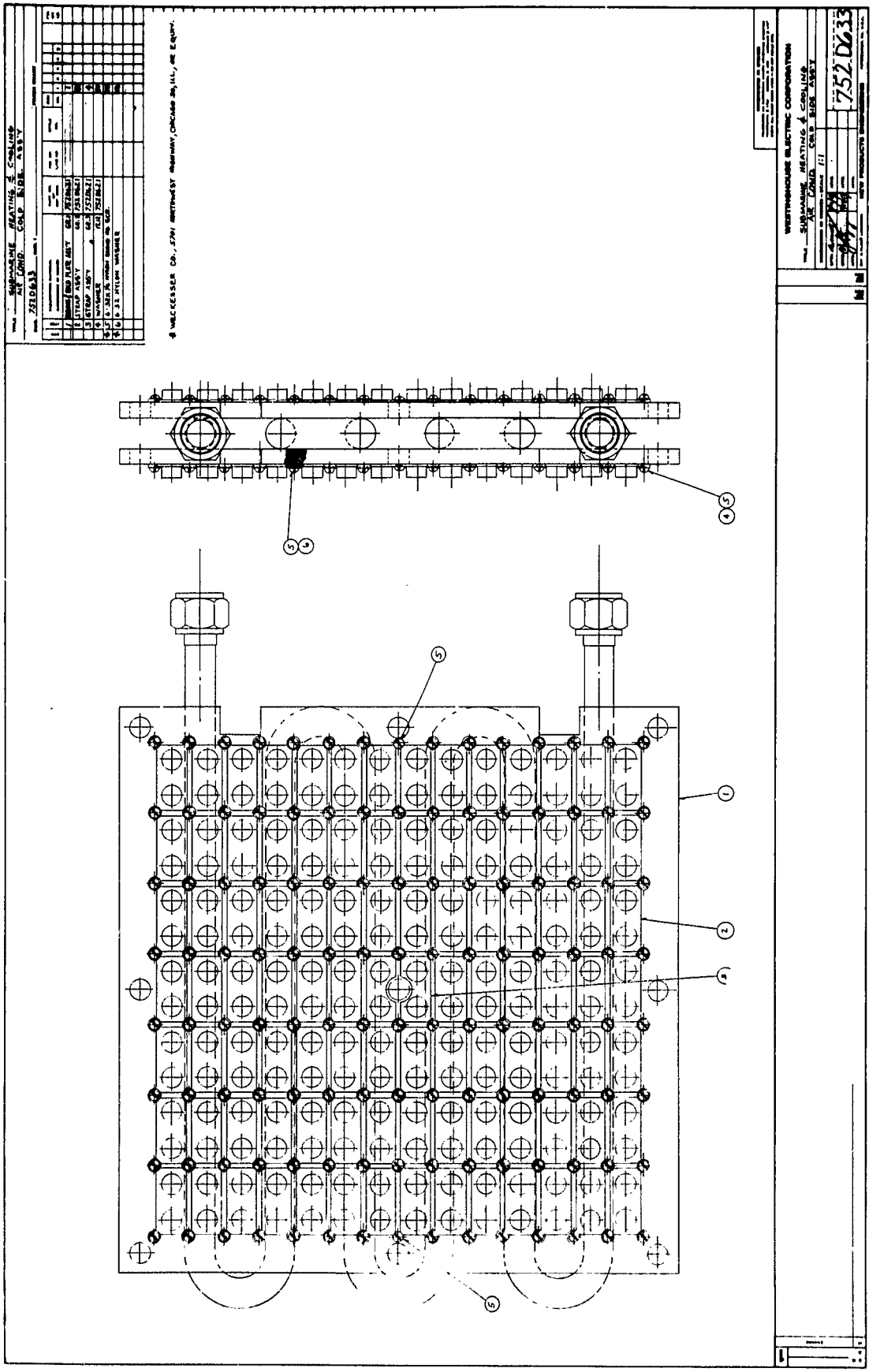

Figure 8 Module 1 Chill Water Heat Exchanger With T.E. Material

N.P.M.-534

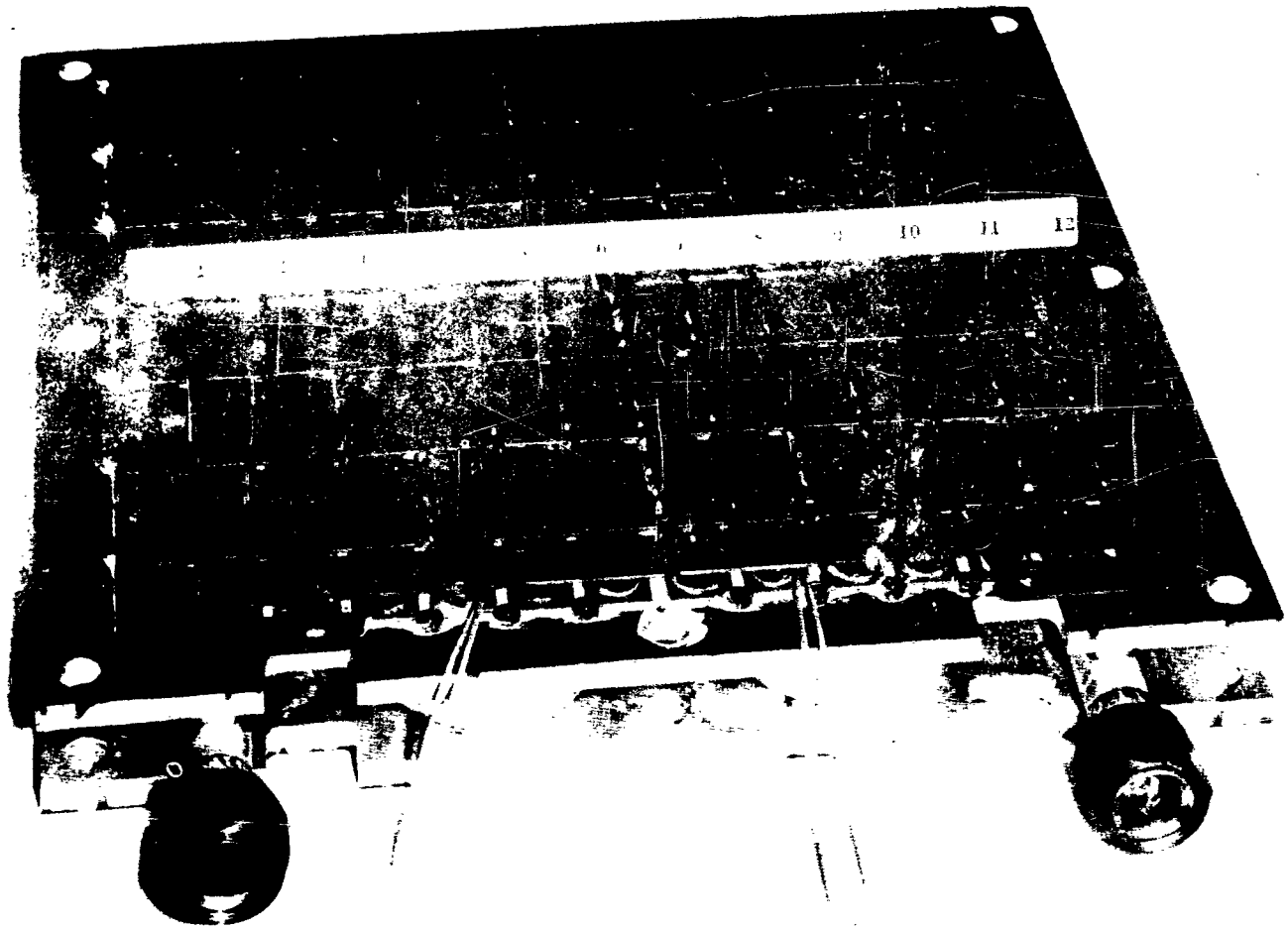

Figure 9 Module 1 Chill Water Heat Exchanger With Straps

an aluminum plate. The details of the construction are shown in Figures 10, 11, and 12. In addition to the fins, heat is extracted along the inside walls of the box which are of aluminum and conducted to the cold plate which is in metal to metal contact with the inside walls. Polyureathane foam is used in the walls of the box for insulation and strength. The area surrounding the thermoelectric pellets is also filled with this foam. There are 50 couples in the unit and the design calculations in Appendix II shown that the unit should operate at 35 amperes and 4.0 volts with a coefficient of performance of 0.32.

In order to demonstrate the cooling and heating capabilities of the thermoelectric module a demonstration system was constructed which consisted of a chill water and a sink water loop. Each loop had a water to air heat exchanger and a water pump. In operation with the module in the loops the air from one heat exchanger became warm and that from the other cool, thus demonstrating the heating and cooling possible with thermoelectrics. A picture of the system is shown in Figure 13.

IV. Module #2 Design

At the time of completion of the first module or prototype the program was re-evaluated and its scope was changed. Instead of continuing with the construction of a 1 ton unit it was decided that one more module would be made with emphasis on reducing size and weight and improved performance. The scope was further extended to include the construction of a third module which was to include a sprayed on copper strap technique which was under development at the time. This third module was also to be a prototype of a shipboard unit.

The same number and size of thermoelectric pellets was used in the second module. It differs mainly in that the tubing coils on the heat exchangers was increased in length and flattened slightly to increase the contact area to the aluminum plates to which they were brazed. This can be seen by comparing Figure 6 and Figure 15. The plates themselves were also made thinner. This in effect was an attempt to improve the performance of the heat exchangers so that there would be less temperature differential between the junction straps and the water. Stainless steel screws with insulating shoulder washers were used to hold the junction straps to the chill heat exchanger instead of nylon screws as they could be fastened tighter. This is shown in Figure 14. A polyureathane foam was used around the thermoelectric material as it had been found that the silica aerojel had a tendency to dry out the aluminum oxide paste beneath the junction straps. Thermoelectric material with an average figure of merit of 2.41 x 10^{-3} 1/C° was used which was somewhat higher than the 2.28 x 10^{-3} 1/C° of the first module. In addition to making the heat exchangers lighter, a reduction in weight and size, was also obtained bringing the water connections from each heat exchanger to the outside of the unit. This can be seen in Figures 15 and 16 which shows the completely assembled module.

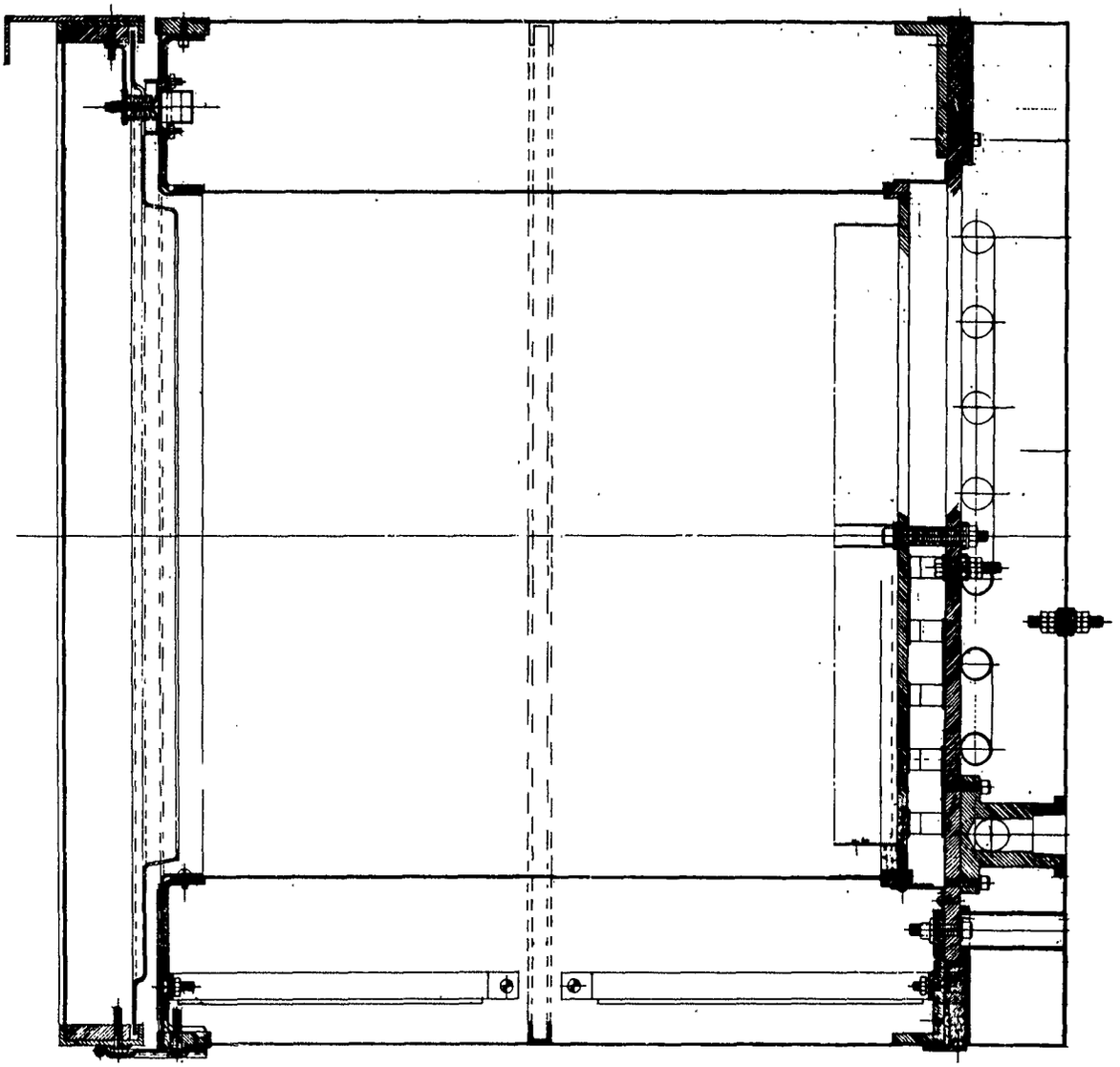

Figure 10- Freezer Cross Section View

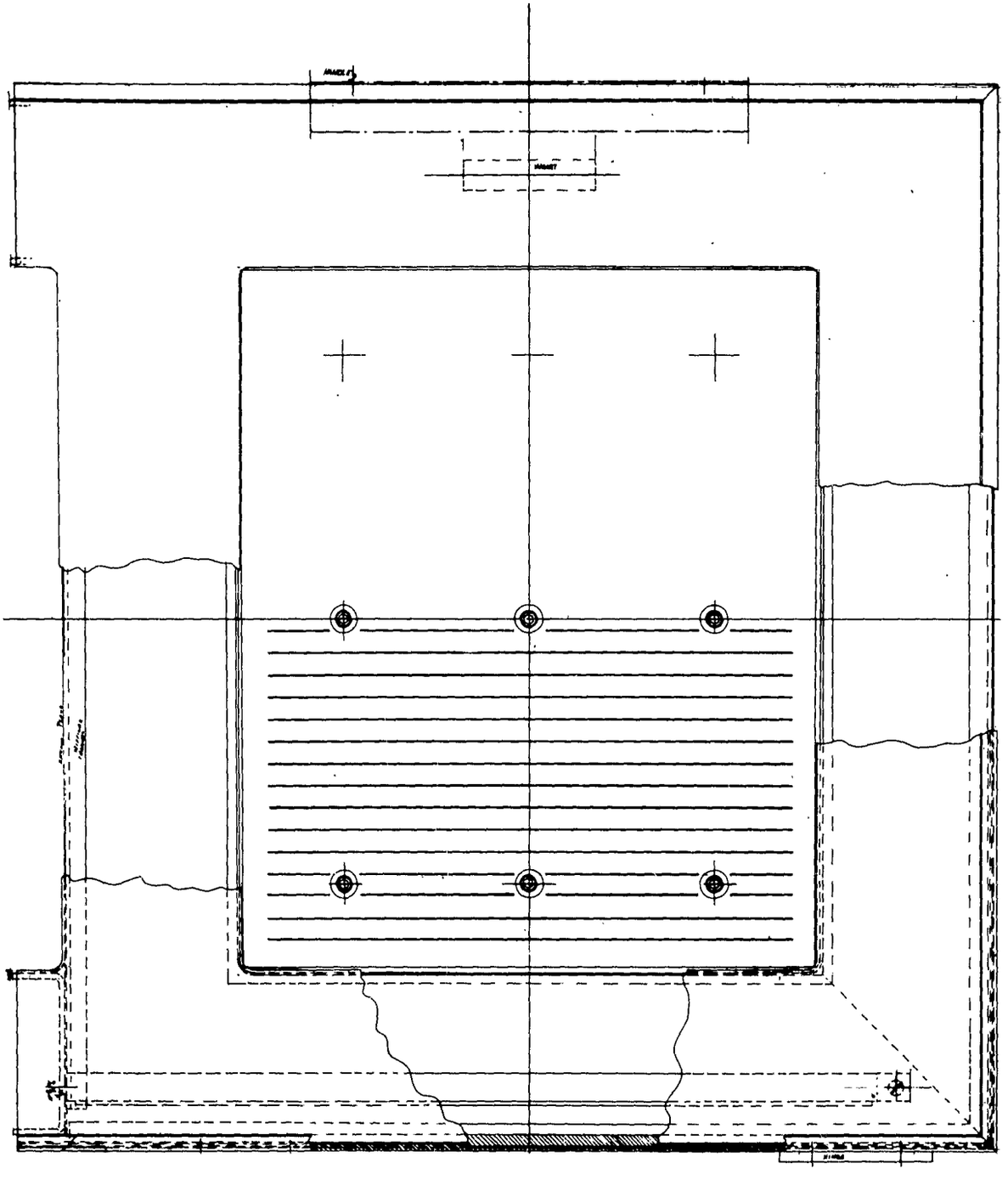

Figure 11 Freezer Front View

Figure 12 Freezer With Door Open

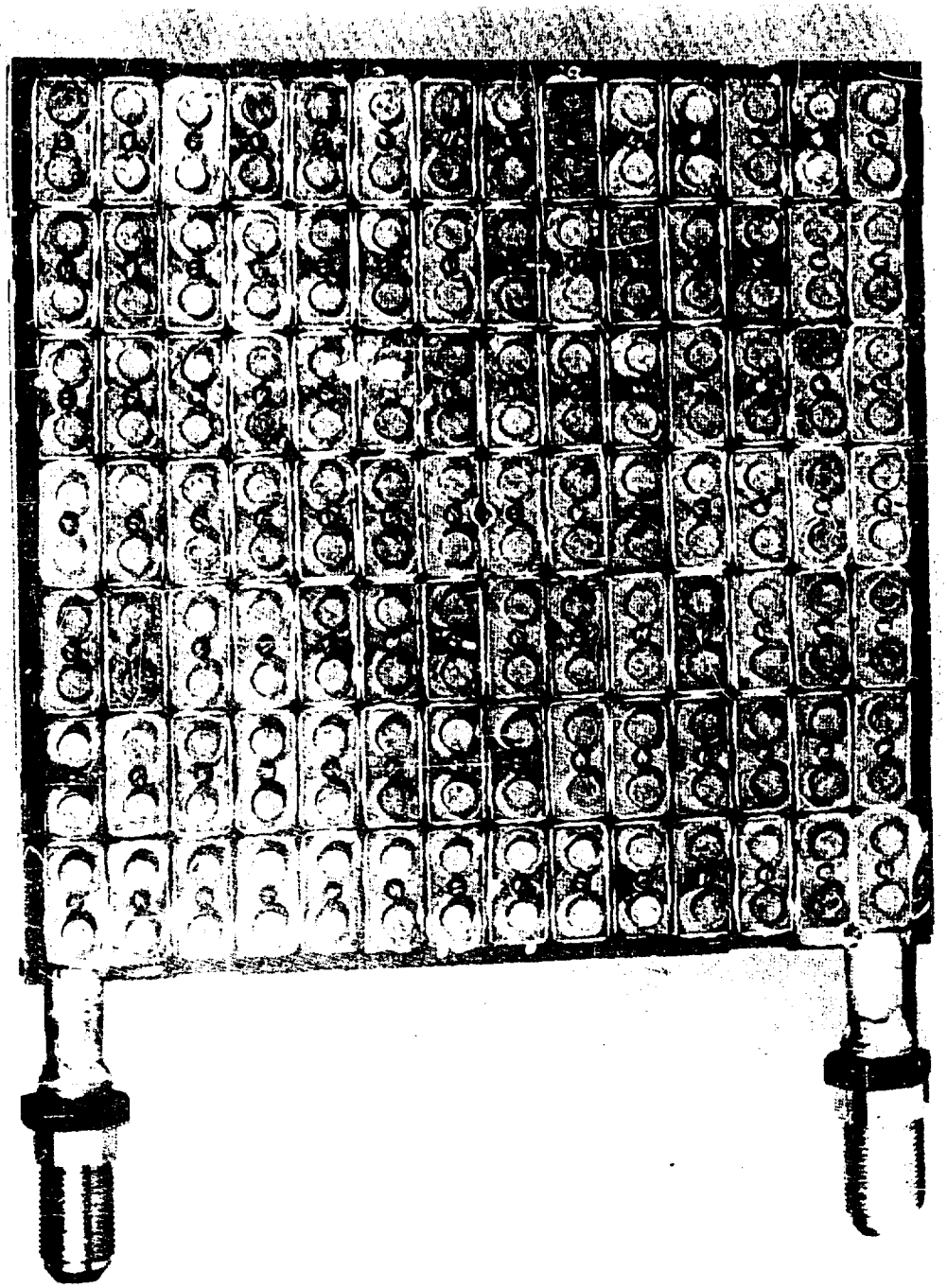

Figure 14 Module 2 T.E. Pellet Assembly

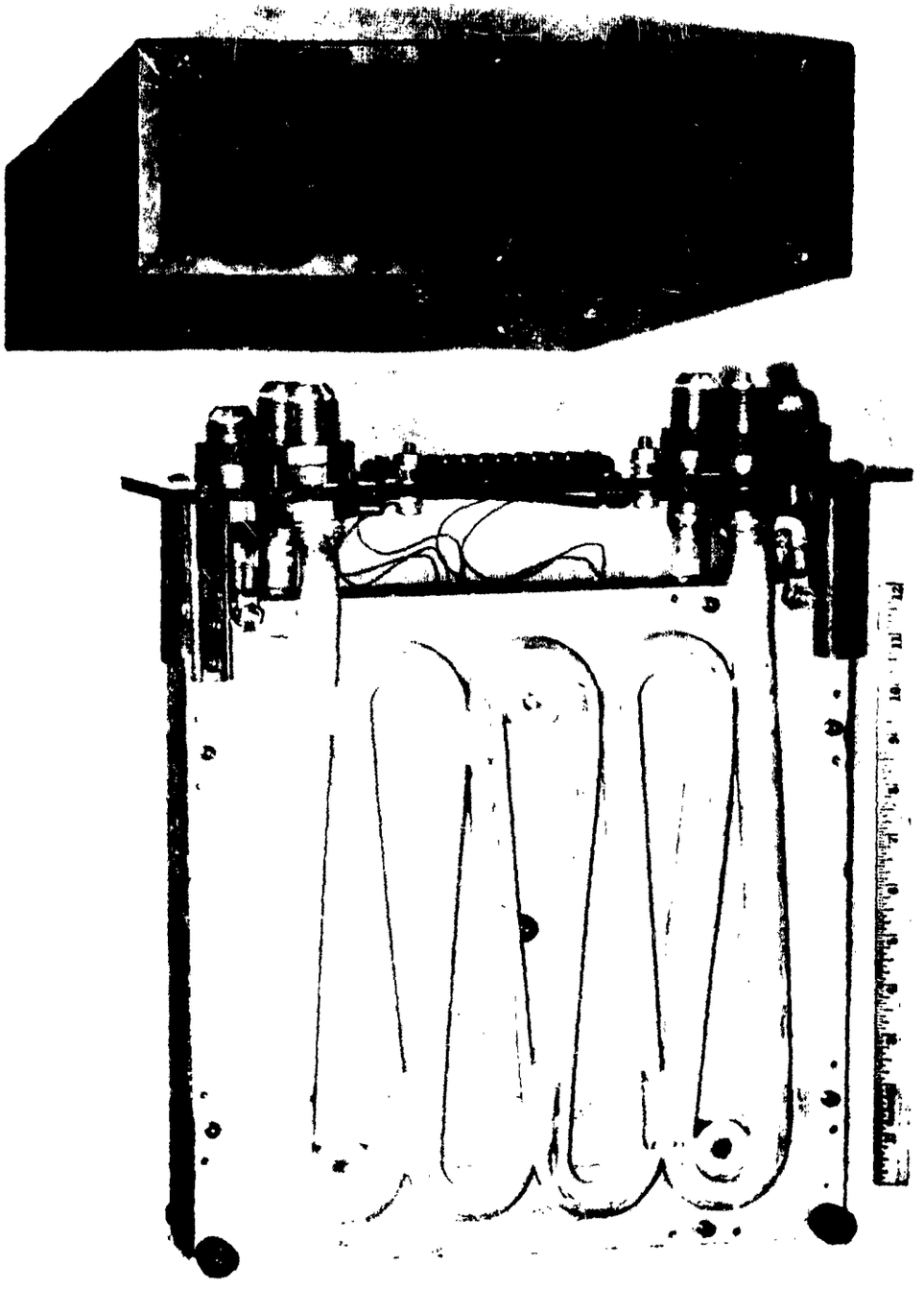

Figure 15 Module 2 Assembly Showing Coiled Tubes

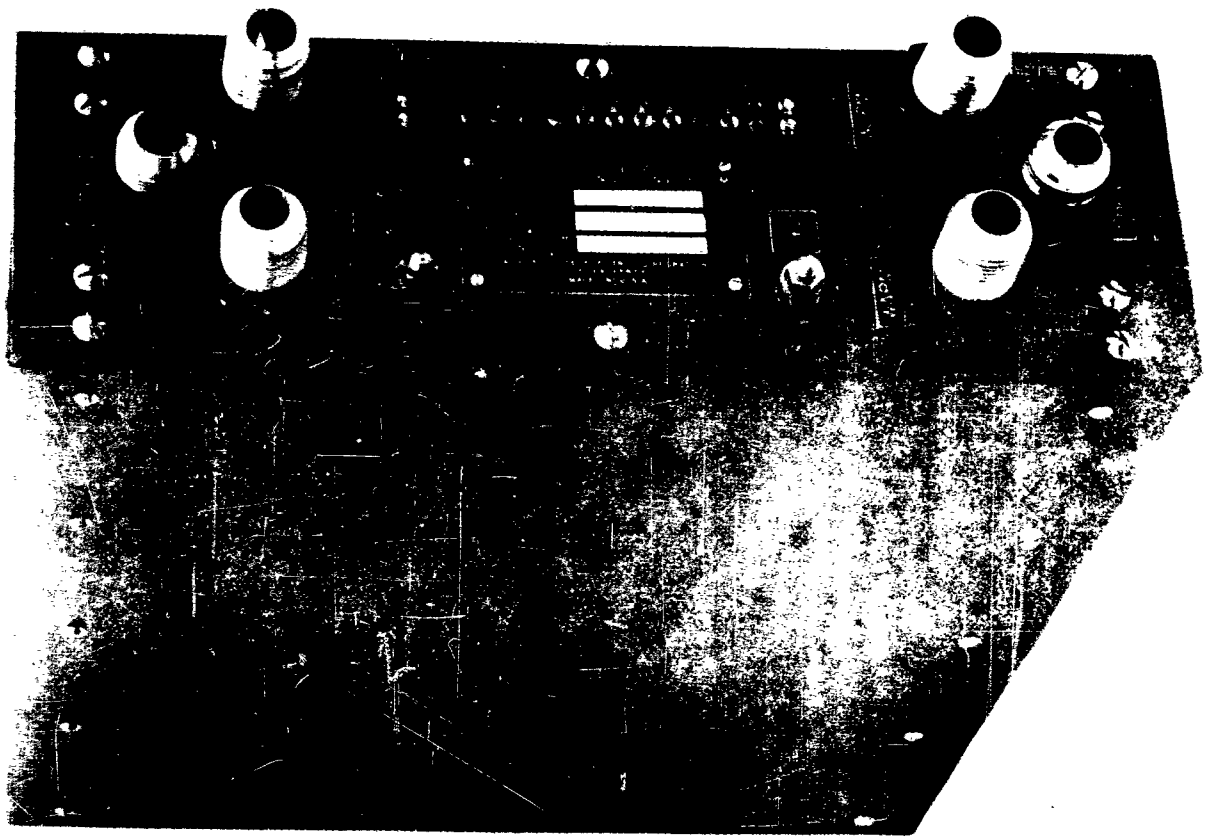

V. Module #3 Design

This unit which was to be a shipboard design was quite different from the previous units. The experience gained on the previous modules indicated that heat exchangers which could remove the heat with very little temperature differential would greatly increase the performance. To this end the heat exchangers were then constructed by casting aluminum around a coiled tube. The aluminum around the tubing providing a good thermal conducting path and also a flat surface on which the thermoelectric couples could be assembled. Further improvement in the heat exchangers was obtained by increasing the length of tubing. This was done by obtaining very small radius 180° end bends which were brazed on as shown in Figure 17. The increase in length of tubing however was gained at the expense of pressure drop of the water through the tubing. It was felt the improvement in performance would outweigh the loss introduced by the increased pressure drop. The cast in aluminum heat exchangers are shown in Figure 18. The water inlet and outlets or headers were constructed so that no external water cross connections are required in the module or between other modules of the same design. This was accomplised as shown in Figure 19 by the use of "0" ring sealed connections between headers. In addition, this design permitted the water flow to be arranged in either series or parallel flow or various combinations of flow through both chill and sink heat exchangers when more than one module was used. This type of construction made the external outline of a module to be simple a box, 1 foot by 1 foot by 3 inches and the stacking of several modules together could be done in the minimum of space. All of the heat exchanger tubing and headers were constructed of 10-90 cupro-nickel for good salt water corrosion resistance and all tubes were of sufficient strength to withstand submergence pressures. Efficient heat exchangers were required for two reasons, to improve performance of the thermoelectric material, and to remove the additional heat introduced by the increase in the packing factor gained by the use of the sprayed on junction strap technique. With an increase in the number of couples per square inch more heat must also be removed per square inch.

The increased packing factor of thermoelectric material was obtained by the spraying the hot junction straps onto the sink heat exchanger. This technique allows closer packing as no additional fastening devices are required to hold the strap in place, and as better thermal conduction to the heat exchanger is obtained by intimate contact between the strap and heat exchanger. To obtain electrical insulation, a 5 mil thickness of aluminum oxide is first sprayed on the flat surface of the heat exchanger. Using a grid or matrix of stainless steel which outlines the straps, a layer of aluminum is sprayed on for good adherance to the oxide. Then, a layer of copper is sprayed on to the required thickness. For this module enough metal was sprayed on so that the thickness of the strap after being fly cut to a smooth surface was 0.040 inches. In Figure 20, is shown a heat exchanger after being sprayed and in Figure 21 after it has been machined. Before machining a layer of epoxy resin is painted over the complete sprayed surface. This was done to prevent the soldering flux which was used to tin the straps from soaking into the aluminum oxide and nullifying its electrical insulating properties. The thermoelectric couples were soldered to the straps with the aid of a stiff cardboard matrix shown in Figure 22. This matrix was positioned over the strap

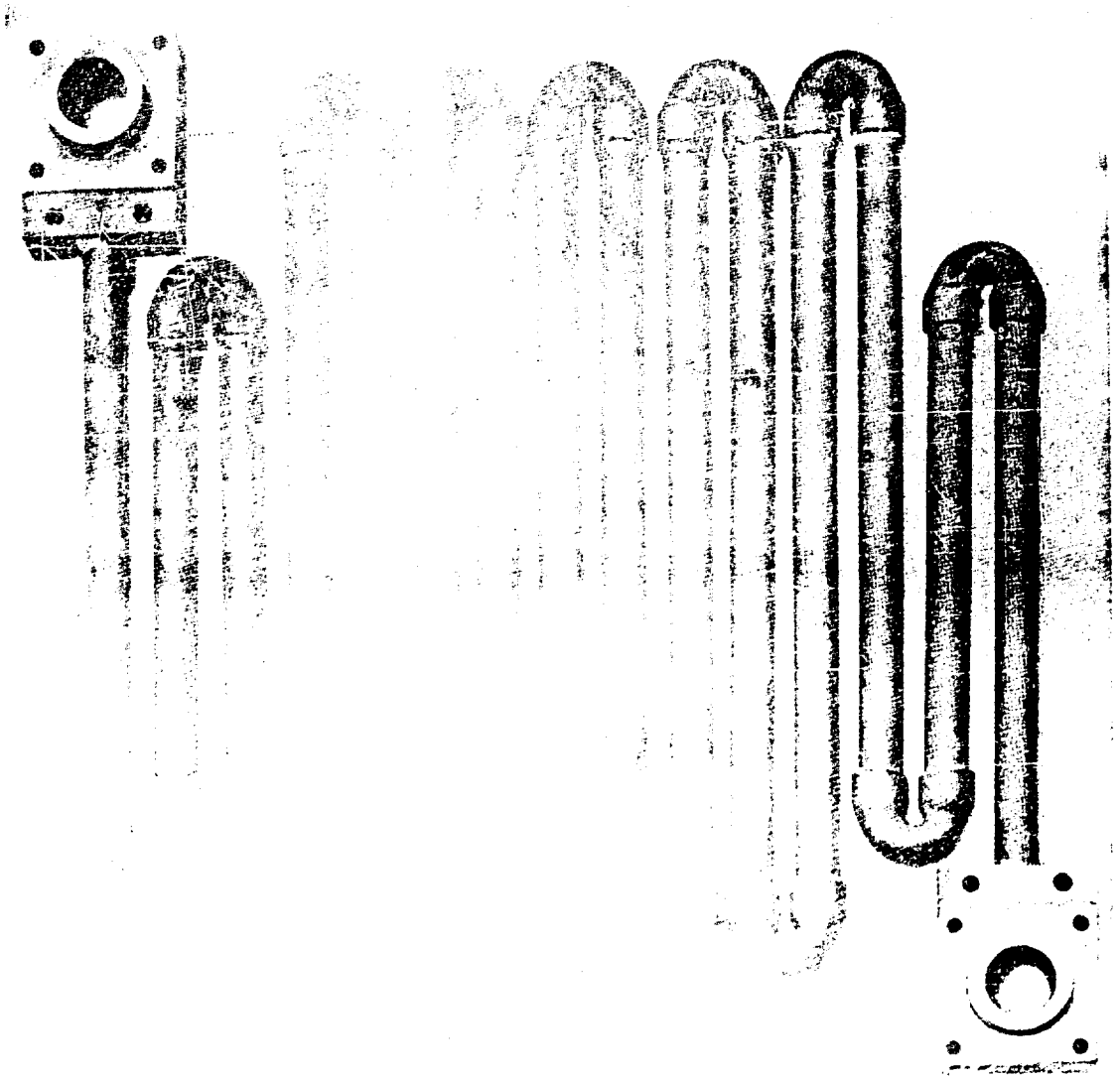

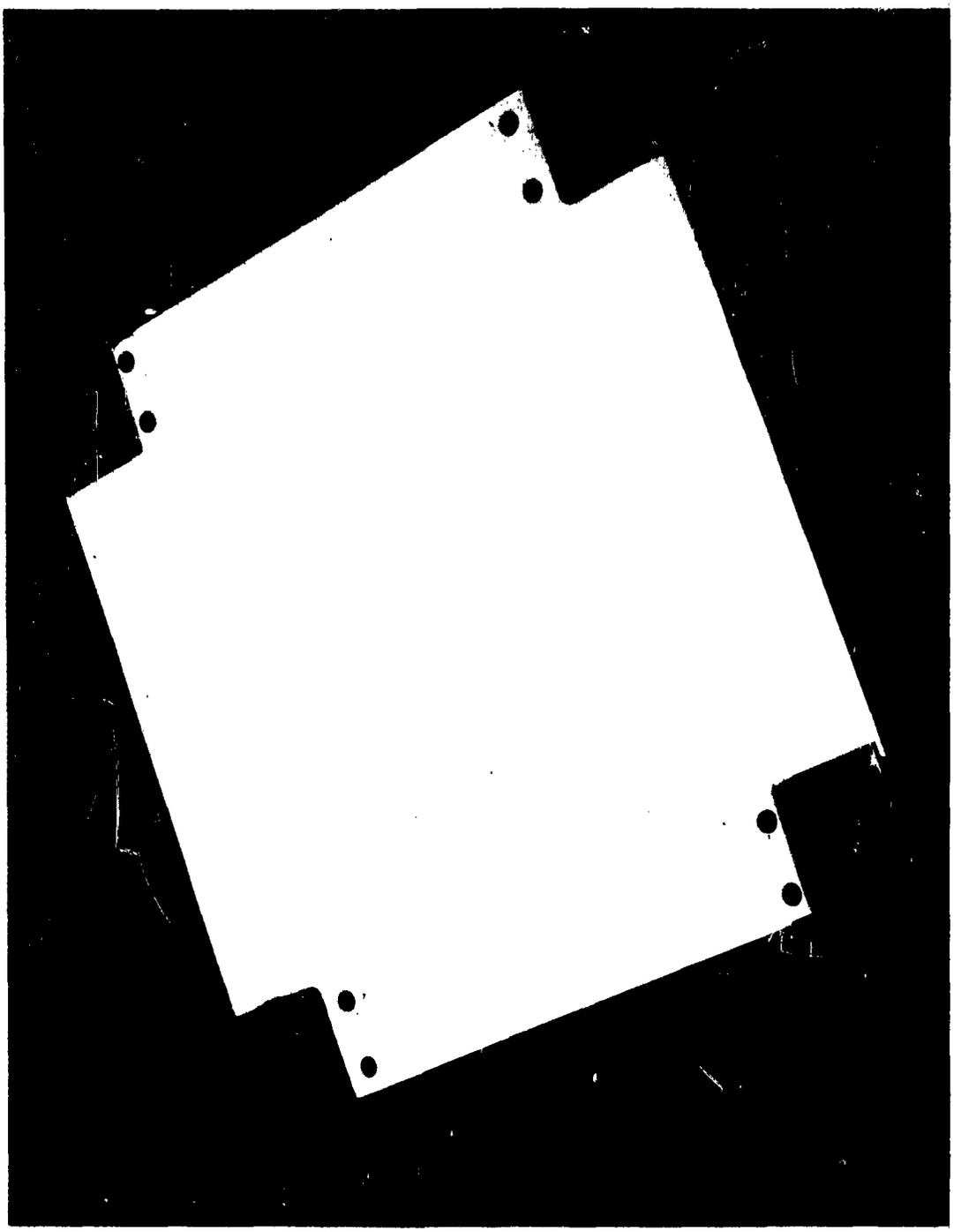

Figure 18 Module 3 Cast Aluminum Heat Exchanger

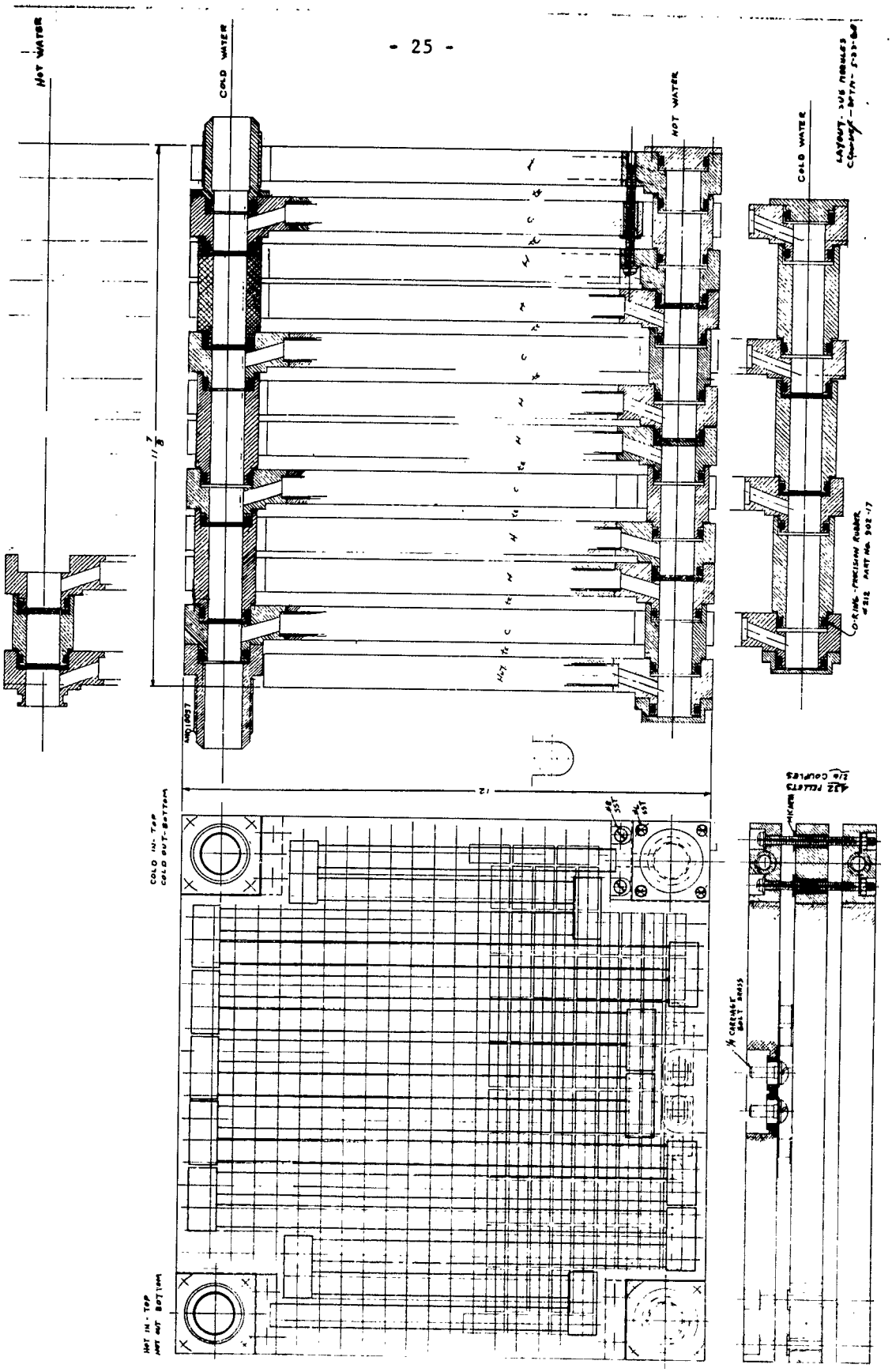

Figure 19 Module 3 Header Construction

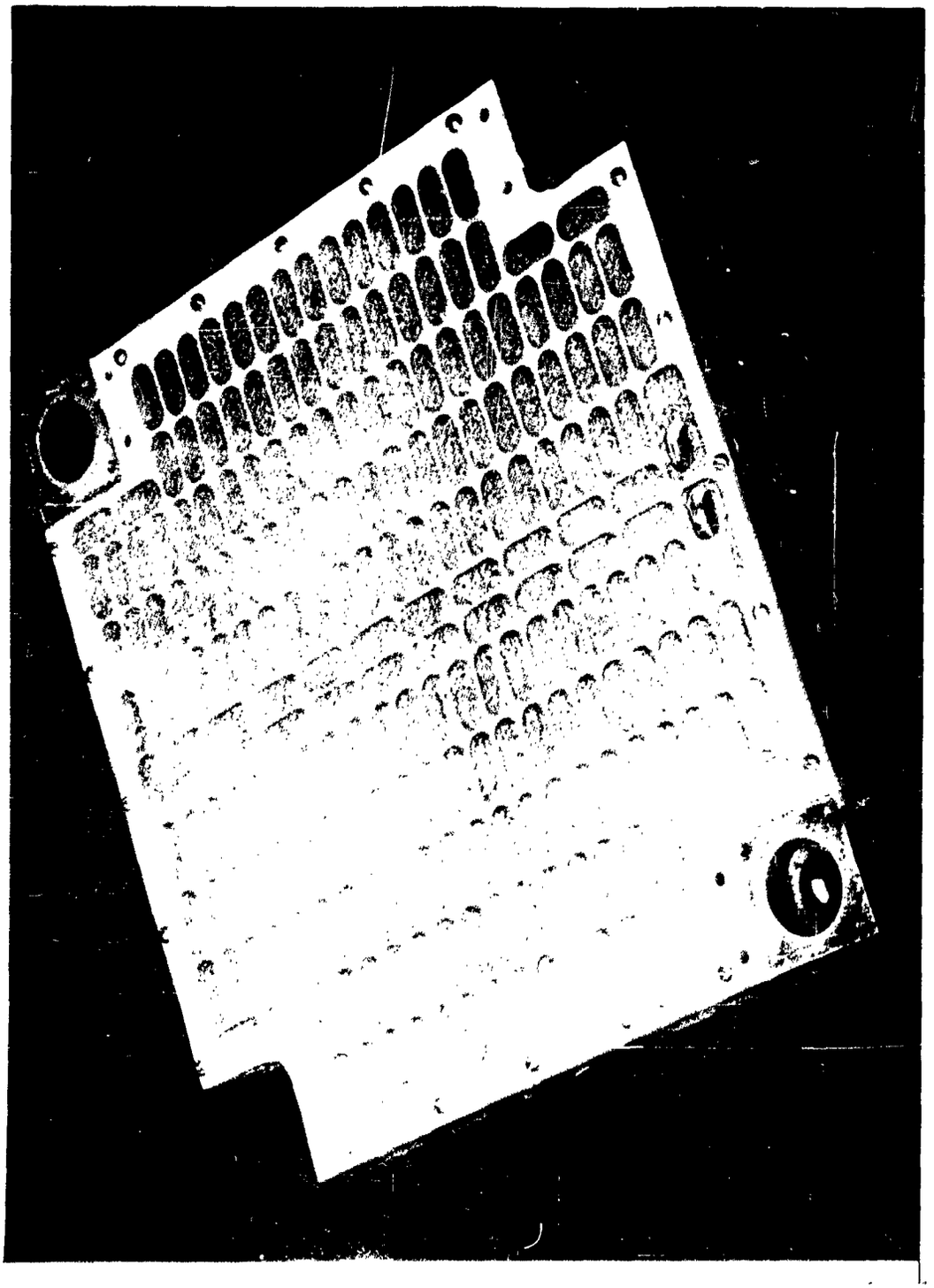

Figure 20 Module 3 Heat Exchanger With Sprayed Straps

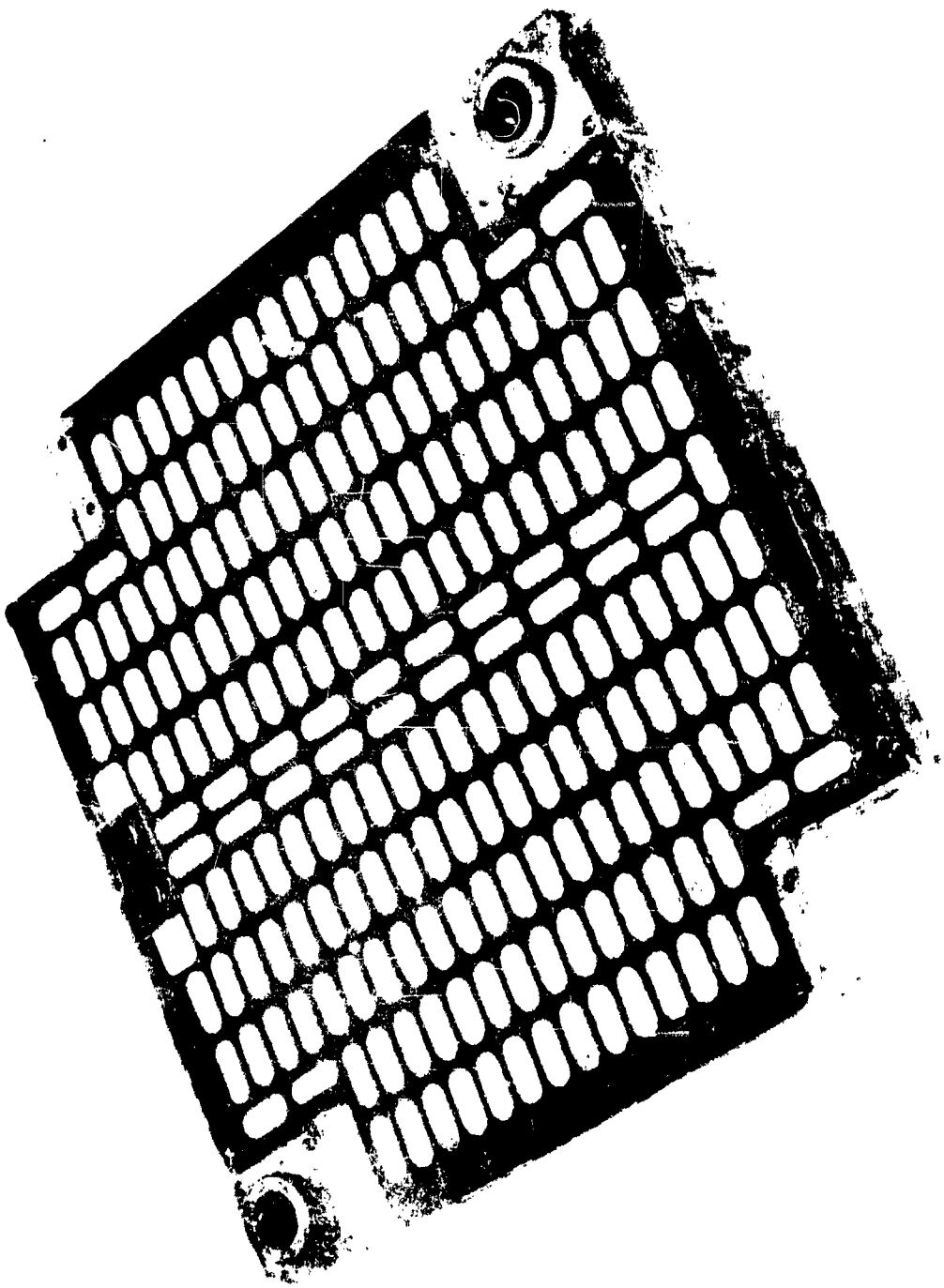

Figure 21 Module 3 Heat Exchanger With Machined Straps

NPM - 1492

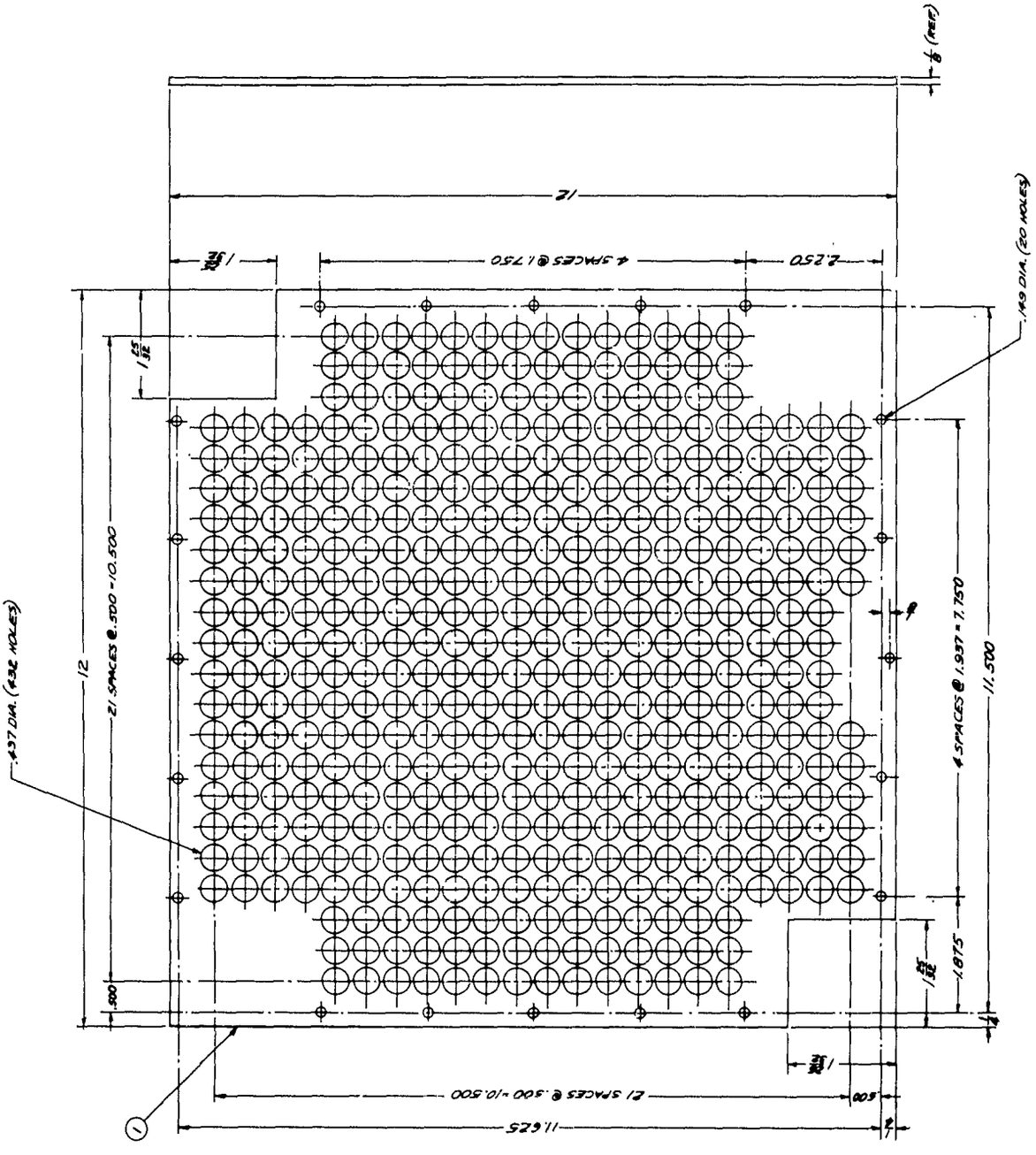

Figure 22 Module 3 Soldering Matrix

area and the pellets were inserted into the holes one by one in correct sequence. A layer of foam rubber was then placed over the exposed couples and weights were applied over the rubber to gently but firmly force the pellets into intimate contact with the junction straps when the heat exchanger was raised to soldering temperature. After cooling, the matrix was removed by soaking in warm water. Figure 23 shows the pellets soldered to the heat exchanger. The cold junction straps were soldered in place using the same method as described previously for soldering the hot junction straps of module 1 and 2. In Figure 24 is shown a heat exchanger with thermoelectric assembly completed. The chill heat exchanger was sprayed with a 5 mil aluminum oxide coating on both sides for electrical insulation. A silicone grease was also applied to the surface for good thermal contact. As in the previous units the chill heat exchanger was sandwiched in between the two sink heat exchangers and held together by two 1/4-20 high strength bolts in each corner as shown in Figure 25. The bolts went through the chill heat exchanger and are thermally insulated from it by "Micarta"* spacers. The coupling between the two sink heat exchangers was made such that the water flow was in series, although parallel flow could as easily have been obtained. Figure 26 shows the completed module.

VI. Test Procedure

Testing of both modules No. 1 and 2 was accomplished in the same manner. Warm water from the plant supply was circulated through the sink or hot side heat exchangers. After passing through the module, the water was dumped in the plant drain. The cold water for the chill or cold side heat exchanger was also obtained from the plant supply. Here again, the water was thrown away after passing through the module. The heat pumping capacity of the module was determined by measuring the temperature differential between the incoming and outgoing chill water. For the heat pumping capabilities of the modules this temperature differential was relatively small and of the order of one half to two degrees Fahrenheit. To measure this difference accurately, two differential thermometers were used, one in the inlet line and one in the outlet line. These thermometers were graduated to read to 0.01°C and could be estimated to the third decimal point. Before starting the test the two thermometers were calibrated together in a common water bath of approximately the temperature of the chill water. Their difference in readings was recorded and was used as a correction factor in obtaining the true temperature differential. After calibration, the thermometers were placed in wells in the piping as close to the inlet and outlet of the module as was physically possible. The test was then run by maintaining a constant flow and temperature of the incoming sink and chill water and measuring the temperature differential obtained with various values of input current to the module. The heat pumping capability was then determined in BTU/hr as the temperature differential in degrees Fahrenheit times the water flow in lbs per hour,

$$Q = \Delta T \times \text{Flow Rate}$$

In this manner, a curve was obtained showing heat pumping rate versus current input to the module. The coefficient of performance at each current was readily obtained by measuring the voltage input to the module. The coefficient of

* Micarta reg Ⓦ trade name

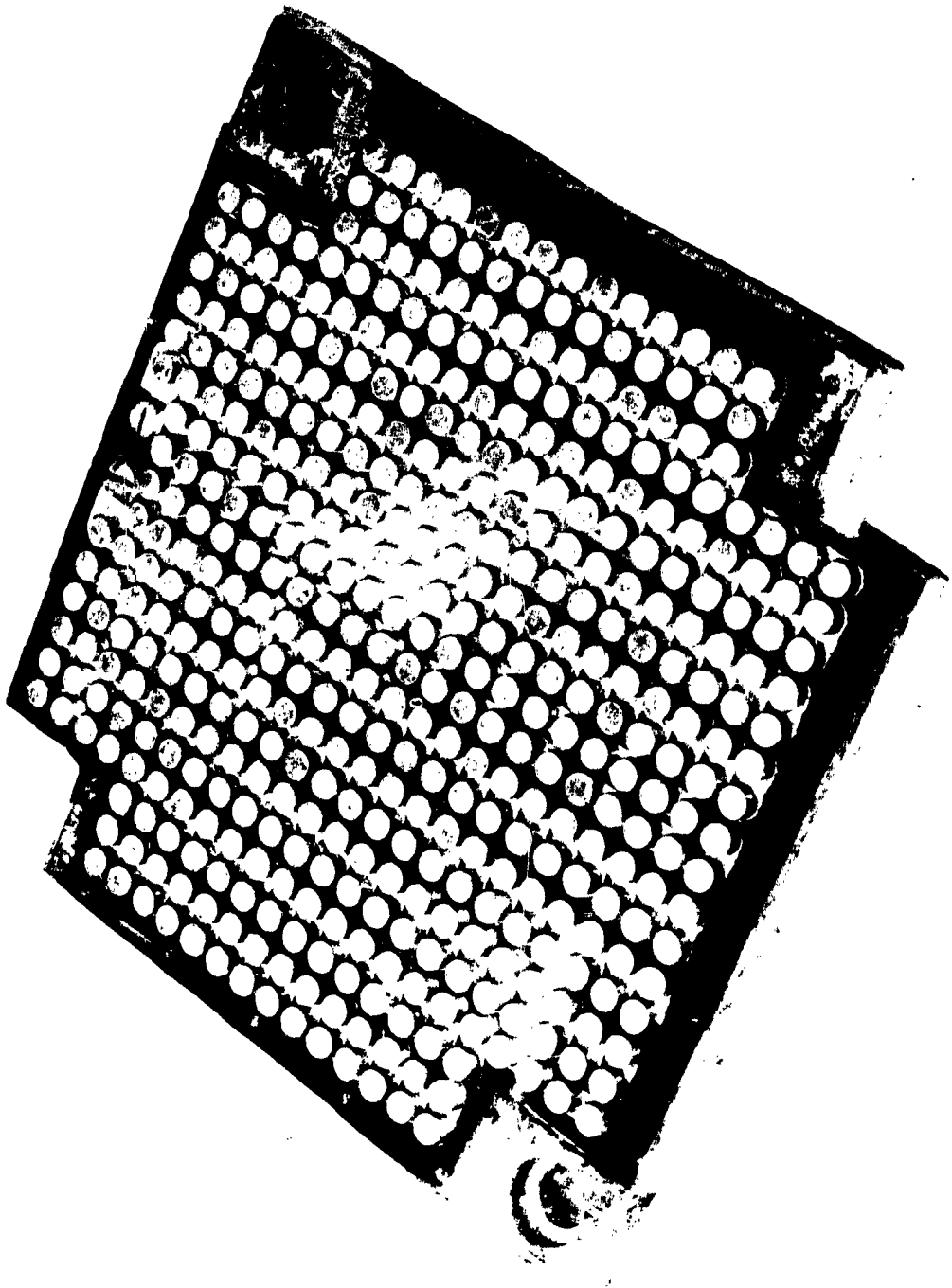

Figure 23 Module 3 Sink Heat Exchanger With T.E. Pellets

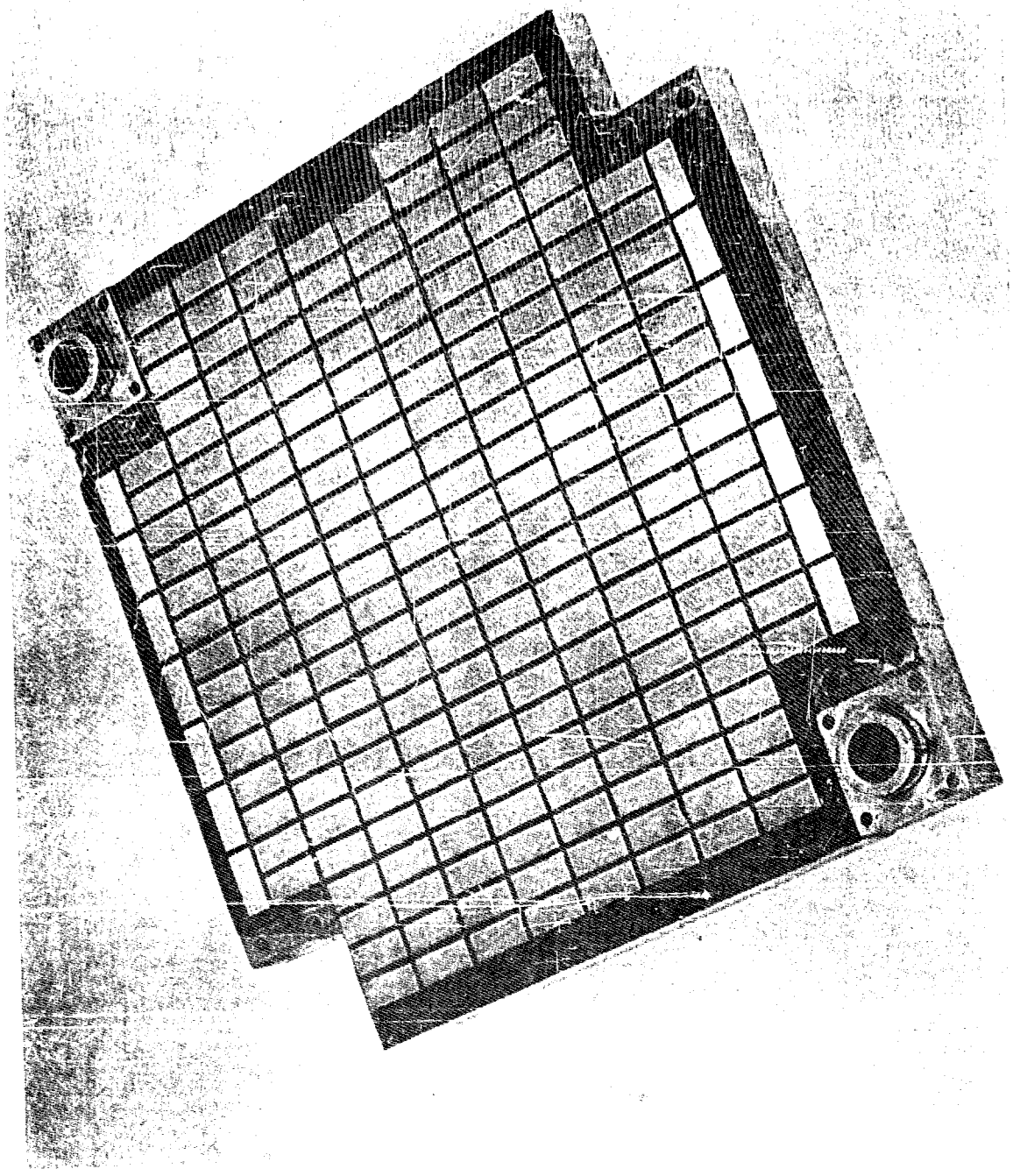

Figure 24 Module 3 T.E. Assembly

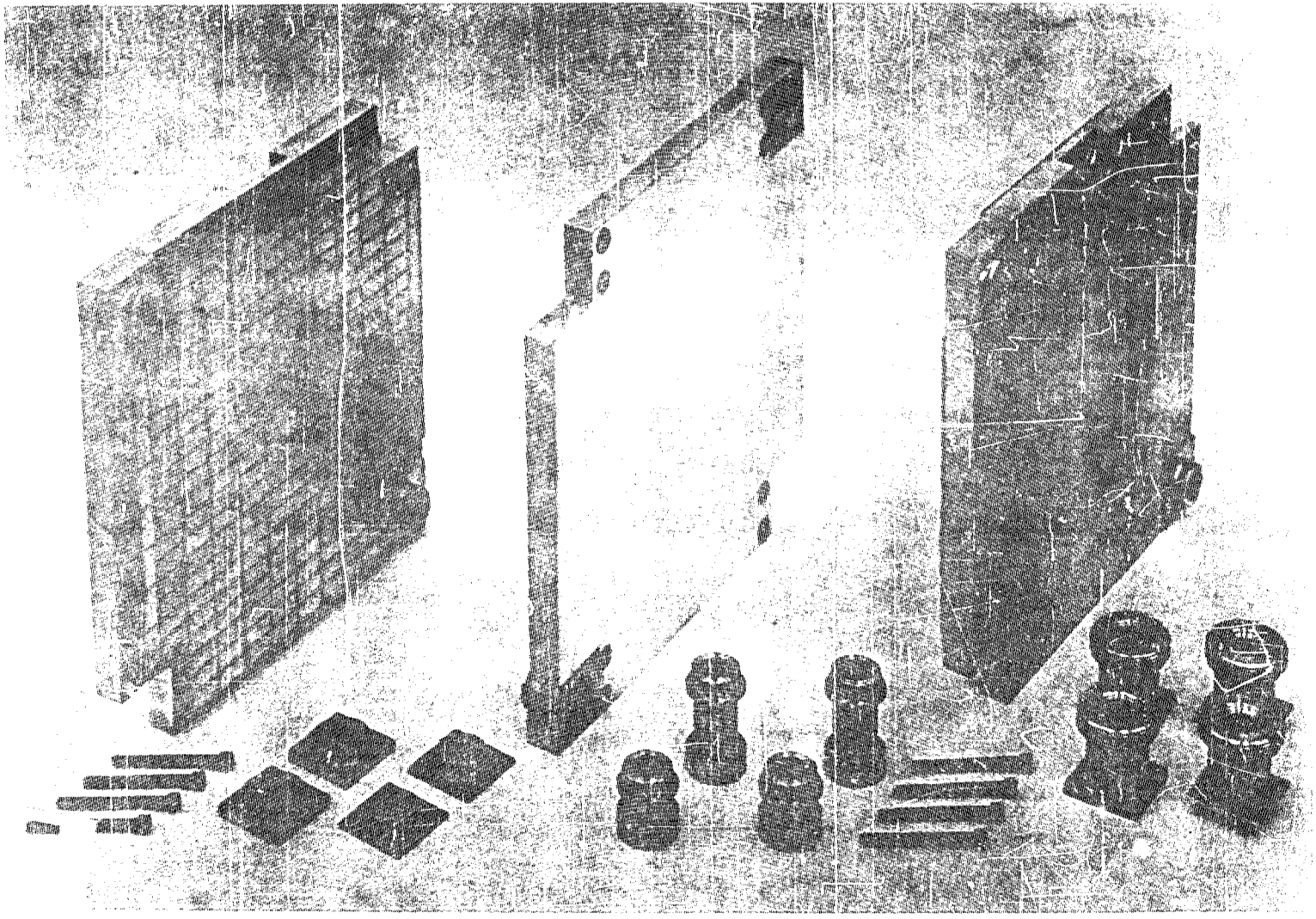

Figure 25 Module 3 Component View

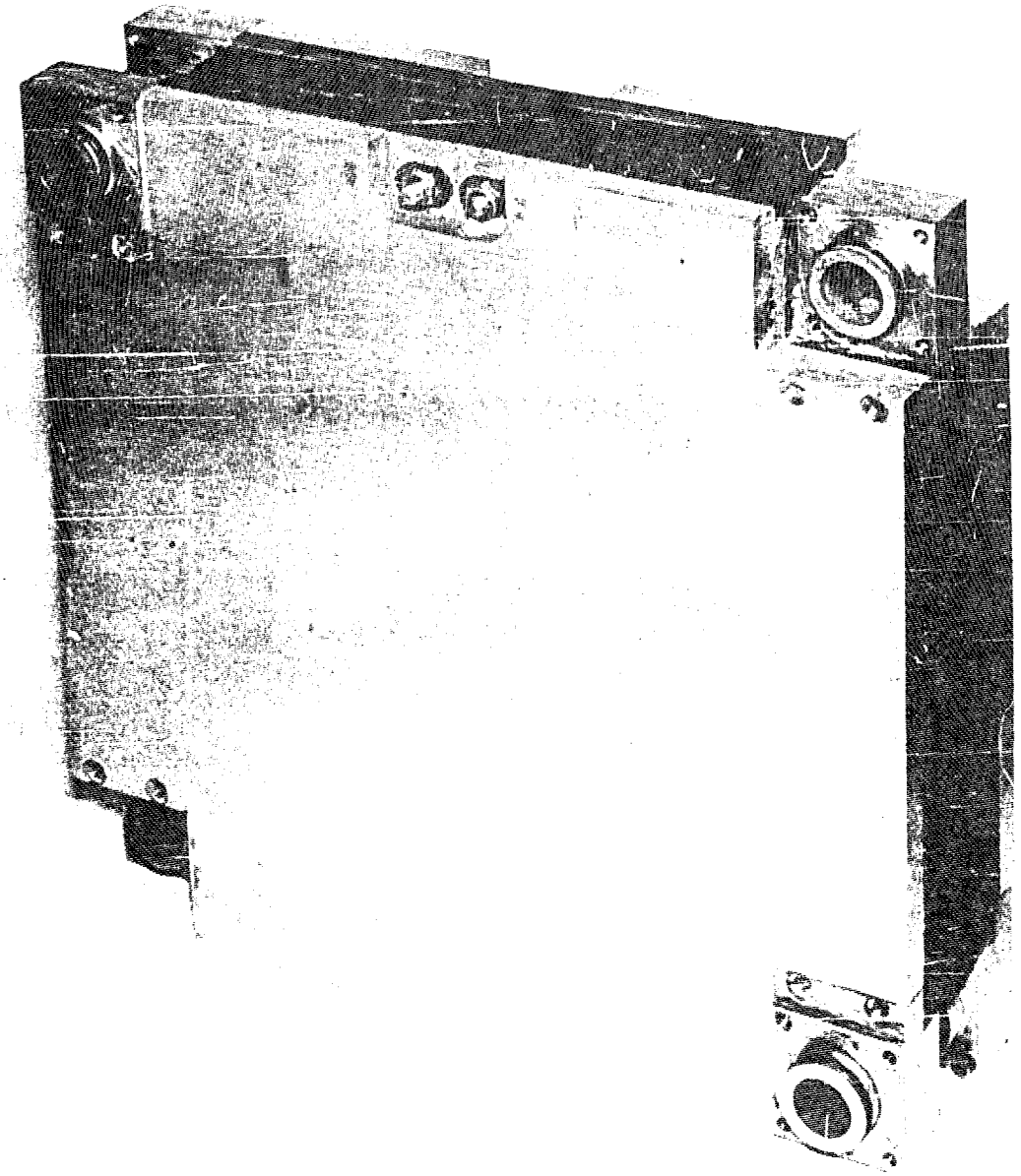

Figure 26 Module 3 Completed Assembly

performance then becomes,

$$C.O.P = \frac{\text{Output}}{\text{Input}} = \frac{Q_{BTU/hr.}}{V \times I \times 3.413\ BTU/hr/watt}$$

This was basically a simple test and could quickly and satisfactorily determine the performance of a module. However, several difficulties were encountered which increased the complexity of the tests. Operating off the plant water supply line, a constant flow and temperature was not obtainable. This was overcome to some extent by making repeated readings at each value of current. Thus, the errors would tend to average out although the time consumed per test was greatly increased. To decrease the time response of the differential thermometers their bulbs were inserted directly in the water flow through rubber packing seals. In the testing of the first two modules this introduced no errors as the pressures involved were very low. As the thermometer bulbs were pressure sensitive this was not satisfactory for testing the third module where the pressure drop across the module was considerably greater.

In testing the this module, the system was changed somewhat. Figure 27 shows the test loops. Both the chill and sink water systems were made closed loops so that their temperature and flow could be controlled more readily. The temperature differential between the entering and leaving chill water was measured in two different ways. Improved thermometer wells were constructed which provided a large contact area between the chill water and the well. The thermometers sat in the wells under atmospheric pressure and were thus not effected by the pressure in the chill water loop. A small amount of water was placed in the wells to provide good thermal contact between the thermometer and the well. Thermocouples were also inserted directly into the inlet and outlet water flow through glass insulated bushings soldered directly in the inlet and outlet fittings. An insulating enamel was sprayed over the thermocouples exposed within the fitting to prevent leakage currents through the water from one thermocouple to the other. The thermocouples as shown in Figure 27 were connected differentially so that their output was a direct measure of the temperature differential between inlet and outlet water. For the range of temperature differentials obtained the thermocouple output was around 100 microvolts and below. This output was measured by a precision Rubicon Bridge and galvanometer. With the aid of the appropriate thermocouple tables, the reading of the bridge was converted to degrees of temperature. A very good agreement between the thermocouples and the differential thermometers was obtained especially at the higher heat pumping rates. Thermocouples were also inserted in the sink loop to determine the amount of heat being dissipated in the sink water. Knowing the input, output, and heat dissipated, a heat balance was obtained which was a good control over the accuracy of the measurements.

Pressure gauges were inserted in the ingoing and outgoing lines to determine the pressure drop through the module at various flows. Flow rates were measured by rotameters inserted in the outgoing lines. Although the flowmeters were of $\pm$ 2

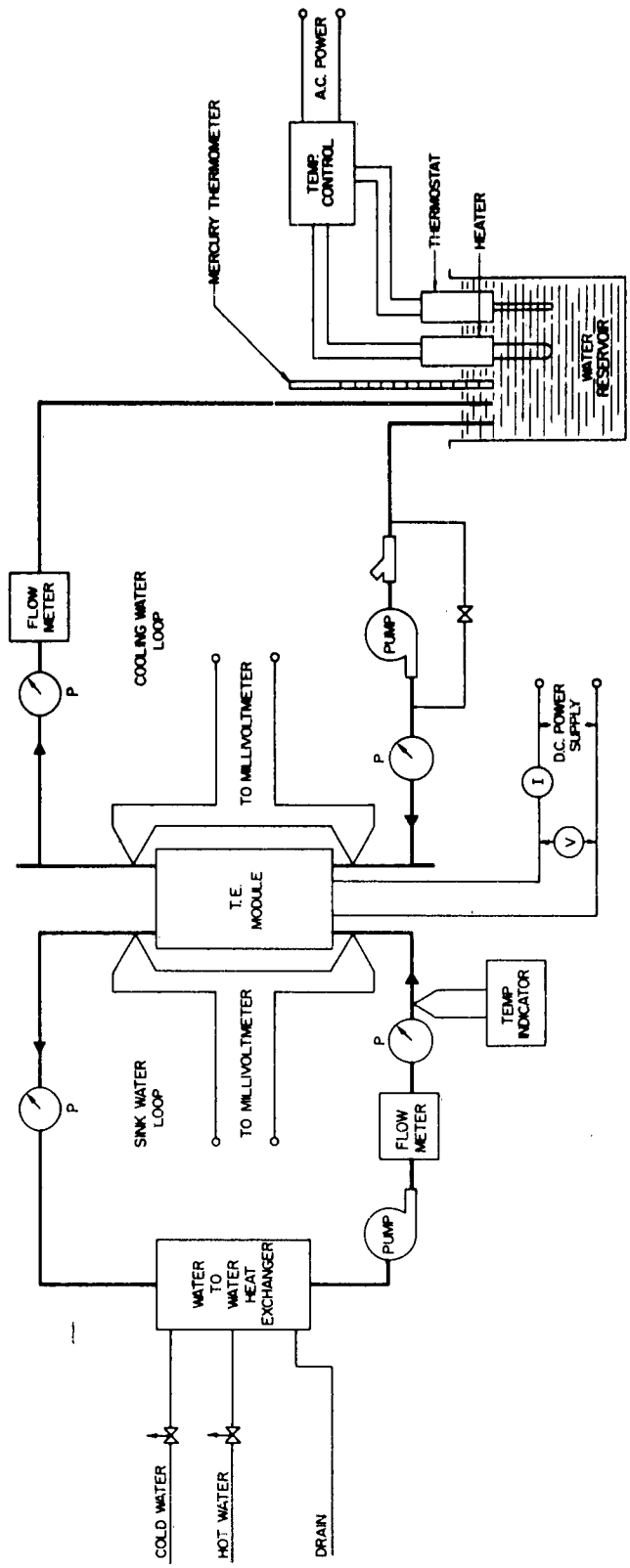

FIG. 27- THERMOELECTRIC MODULE TEST LOOPS

per cent accuracy they were calibrated by weighing a timed flow to an accuracy of ± 1/2 per cent. Measurement of the sink and chill water temperatures were made with thermometers with an accuracy better than ± 1/2 per cent. Voltage and current were also measured using instruments of ± 1/2 per cent accuracy.

As shown in Figure 27, the temperature of the chill water was maintained constant at the desired value by adding heat electrically to the water in the chill water reservoir. This control was maintained automatically within a 0.1°F by an electronic temperature controller which turned a portion of the heat on and off as required. The sink water heat exchanger was held constant by a water to water heat exchanger which extracted heat from the sink water loop. The plant water supply was used as the cooling water and its flow was controlled both manually and automatically to maintain the desired sink water temperature.

Pressure testing of the heat exchangers separately and of the completed third module was done statically up to 2000 psi. No noticeable effect was observed from these tests.

Shock and vibration tests were conducted on the third module to MIL-S-901B and MIL-STD-167. Two complete shock tests were made. The first one was run with the same water running through both the chill and sink heat exchangers. The unit was energized at 35 amperes. The second test was run with approximately 85°F water running through the sink heat exchanger and 50°F water through the chill heat exchanger. The unit was again energized at 35 amperes. The vibration test was run with the same temperature water running through both the sink and chill heat exchangers and with an input of 35 amperes. The vibration machine used was not capable of oscillating in the vertical plane so this portion of the test was simulated by mounting the module at 90° to the vibrating table. The results of the tests are included in the appendix.

VII. Test Results

In Figure 28 is shown the typical performance curves obtained for the first module. Disassembly of this unit showed that the silica aerogel used for thermal insulation around the thermoelectric pellets had a tendency to dry out the silicon paste used underneath the junction straps. The silica aerogel was replaced with polyurethane foam and this improved the performance as shown in the figure. For these tests the flow rates for the chill and sink water was 38 lb/min and 35 lb/min respectively. A shock test and vibration test was also made on this module under non-operating conditions. Although several junctions broke during these tests, there was no damage to the thermoelectric material itself. The break in the junction was between the plating and the pellet and we believe was caused mainly by the loosening of the bolts holding the unit together during the tests.

The temperatures shown in Table I are those reached after the operating times indicated. The inside area temperature is the temperature of the air in the center of the box. The lower limit of -30°F represents the lowest temperature reached at this location in an operating device.

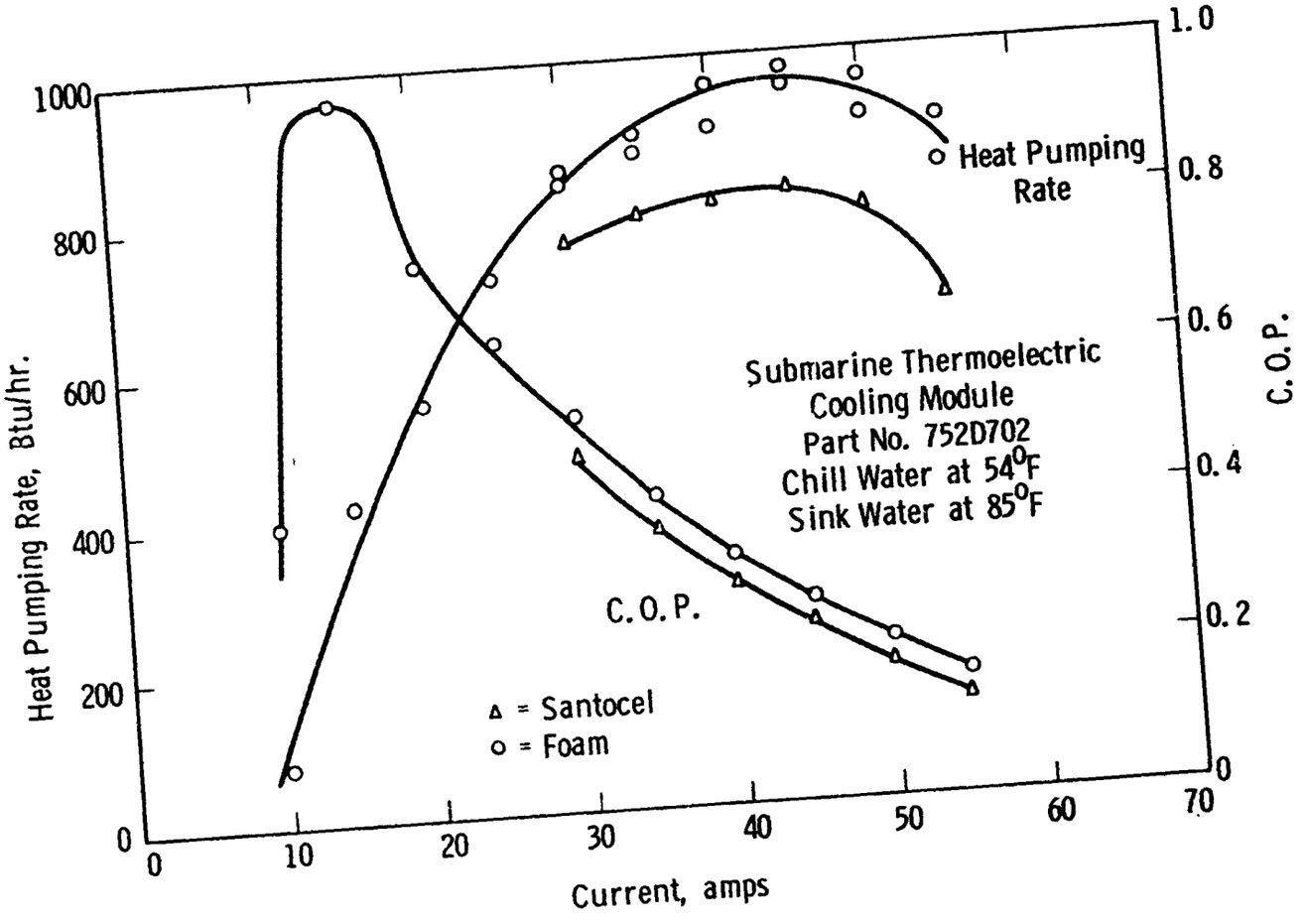

Fig. 28—Module 1 Performance Curves

TABLE I RESULTS OF TEST ON TWO CUBIC FOOT T/E FREEZER

Operating Time - Hrs.	I Amperes	E Volts	P Watts	Inside Area °F	Cold Junction °F	Hot Junction °F
1	40	3.4	136	13	-10	54
1	60	4.9	294	7	-16	55
5+	34	3.05	104	-10	-15	51
5+	40	3.4	136	- 6	-18	54
5+	50	4.1	205	-13	-26	55
5+	60	4.9	294	-16	-30	55

The construction of module two was almost identical to the first except that every effort was made to reduce the size and weight, and to improve the performance by increasing the heat exchanger transfer area and the quality of the thermoelectric material. Using the same number and size of thermoelectric material, the unit weight was reduced from 78 pounds to 38 pounds, and the overall size from 6" x 16" x 19" to 4-3/4" x 15" x 16-1/2" or 1.05 cubic feet to 0.68 cubic feet. Figures 29, 30 and 31 shows the extent to which we were successful in improving the performance of the unit.

As stated previously the third module was to be a prototype of a shipboard installation. Beyond obtaining optimum performance in minimum size and weight the main considerations were that the unit should meet the usual Navy shock and vibration tests and that it should be easily stacked into larger capacity units. The features of this module were, the cupro-nickel cast in aluminum heat exchangers, the sprayed on hot junction copper straps, the headers for ease of stacking, and the use of 432 thermoelectric couples with a Z value of 2.75×10^{-3} 1/°C. The size of the unit was reduced to one foot by one foot by three inches. Although the weight increased to 50 pounds. The performance obtained is shown in Figure 32 for various values of chill and sink water temperatures. The variation of the heat pumping rate with water flow was measured as shown in Figures 33 and 34. The optimum values were then used to run the performance curves. An attempt was made to measure the temperature differential between the junction straps and the chill and sink water. Four copper-constantan thermocouples were placed on various cold junction straps, and four on various hot junction straps. These temperatures were read during the performance tests and the spread of values is shown in Figure 35. The accuracy of these readings is doubtful because of the difficulty in soldering the thermocouples in the correct position.

Since it is necessary to pump both the chill and sink water through module, the pressure drop across the module is a measure of the energy expended in doing so. This pressure drop represents a loss which directly subtracts from the performance of the module as it adds heat to the water. The variation of the pressure drop with various flows is shown in Figure 36 for both the chill and sink water heat exchangers The sink water pressure drop is approximately twice the chill water pressure drop as the sink heat exchanger is essentially two chill heat exchangers.

The witnessed results of both the shock and vibration tests of the third module are shown in Appendix III and IV. No effects due to the tests were noted either during or after the tests. A check of the heat pumping performance was made after the tests and no change was observed.

VIII. Conclusions

The end result of this contract has been the construction of a thermoelectric air conditioning unit which could be used aboard a submarine using a water-to-water type of air conditioning system. This unit is rated at 2550 BTU/hr at a coefficient of performance of 0.75under the conditions of 85°F sink water and 55°F chill water. The direct current which must be supplied to the unit for this performance is 35 amperes with a ripple content less than 5 per cent.

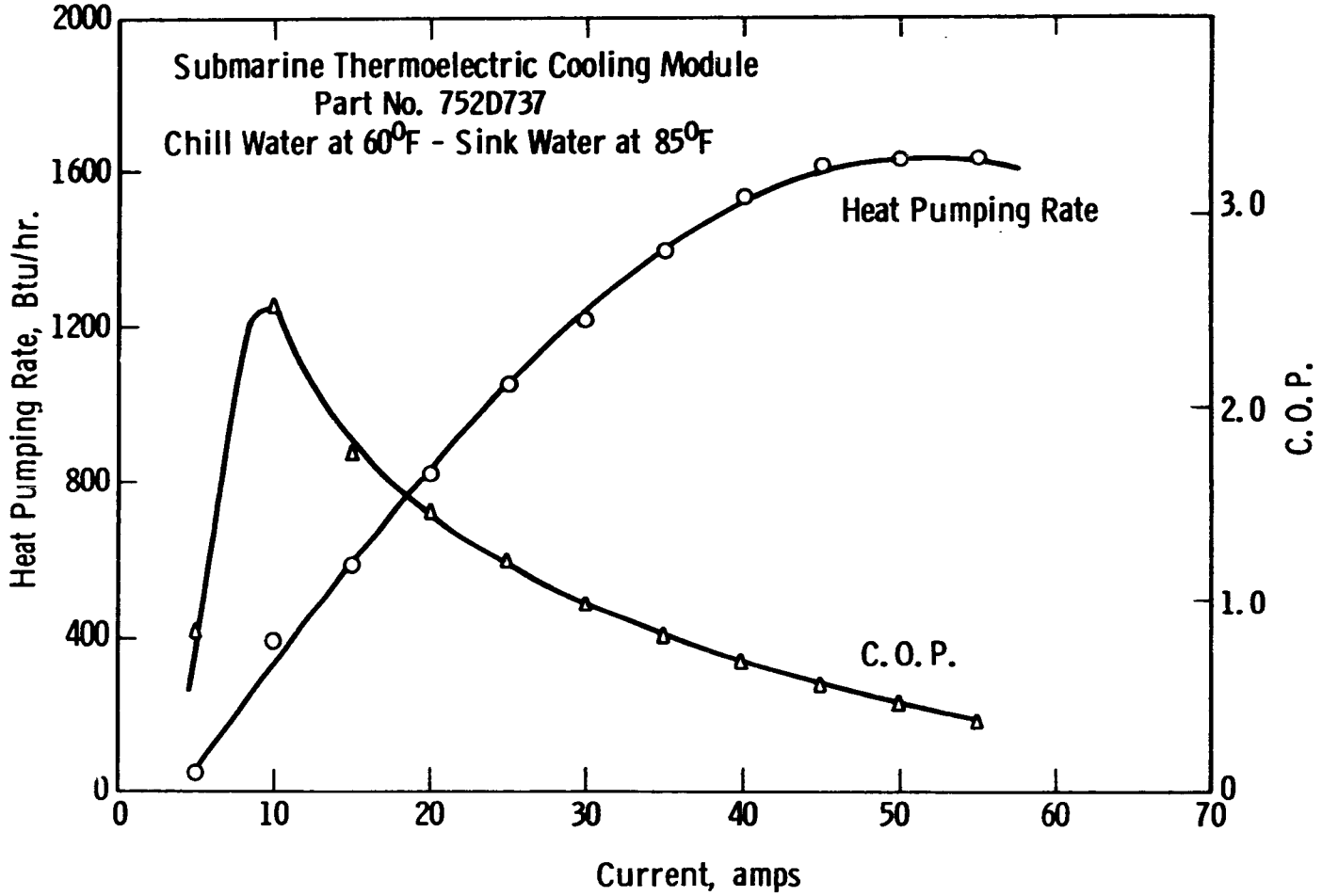

Fig. 29—Module 2 Performance Curves

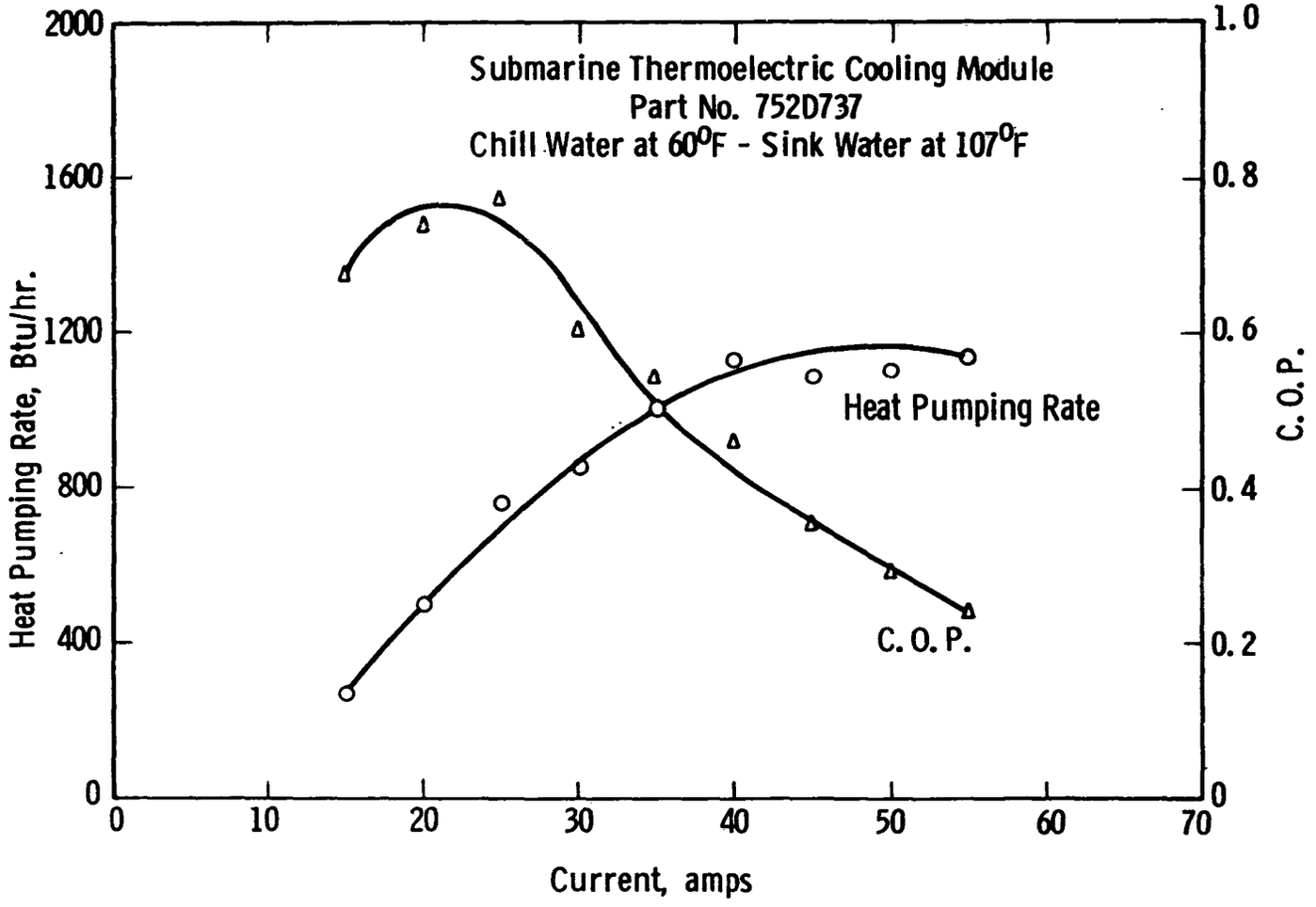

Fig. 30—Module 2 Performance Curves

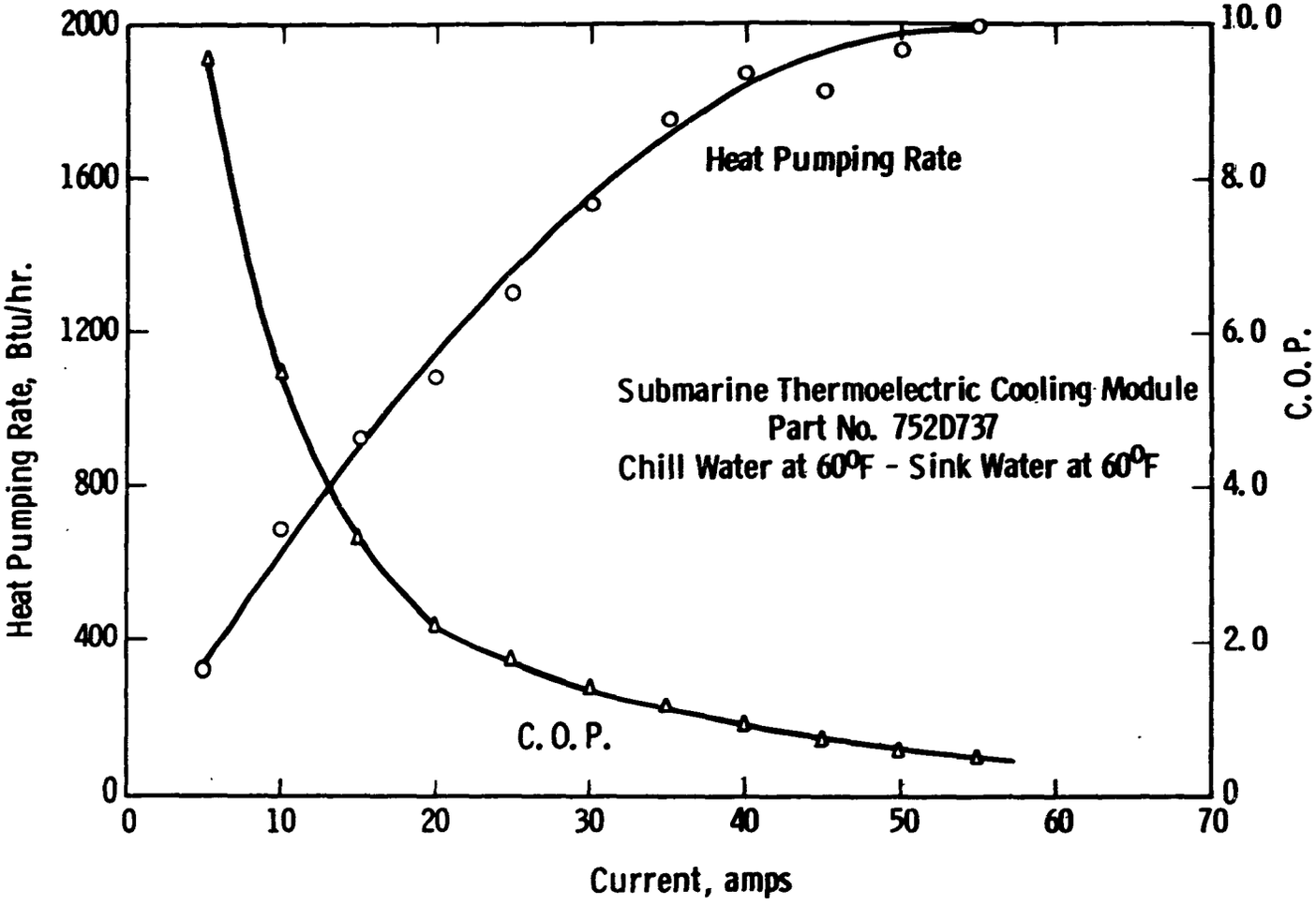

Fig. 31—Module 2 Performance Curves

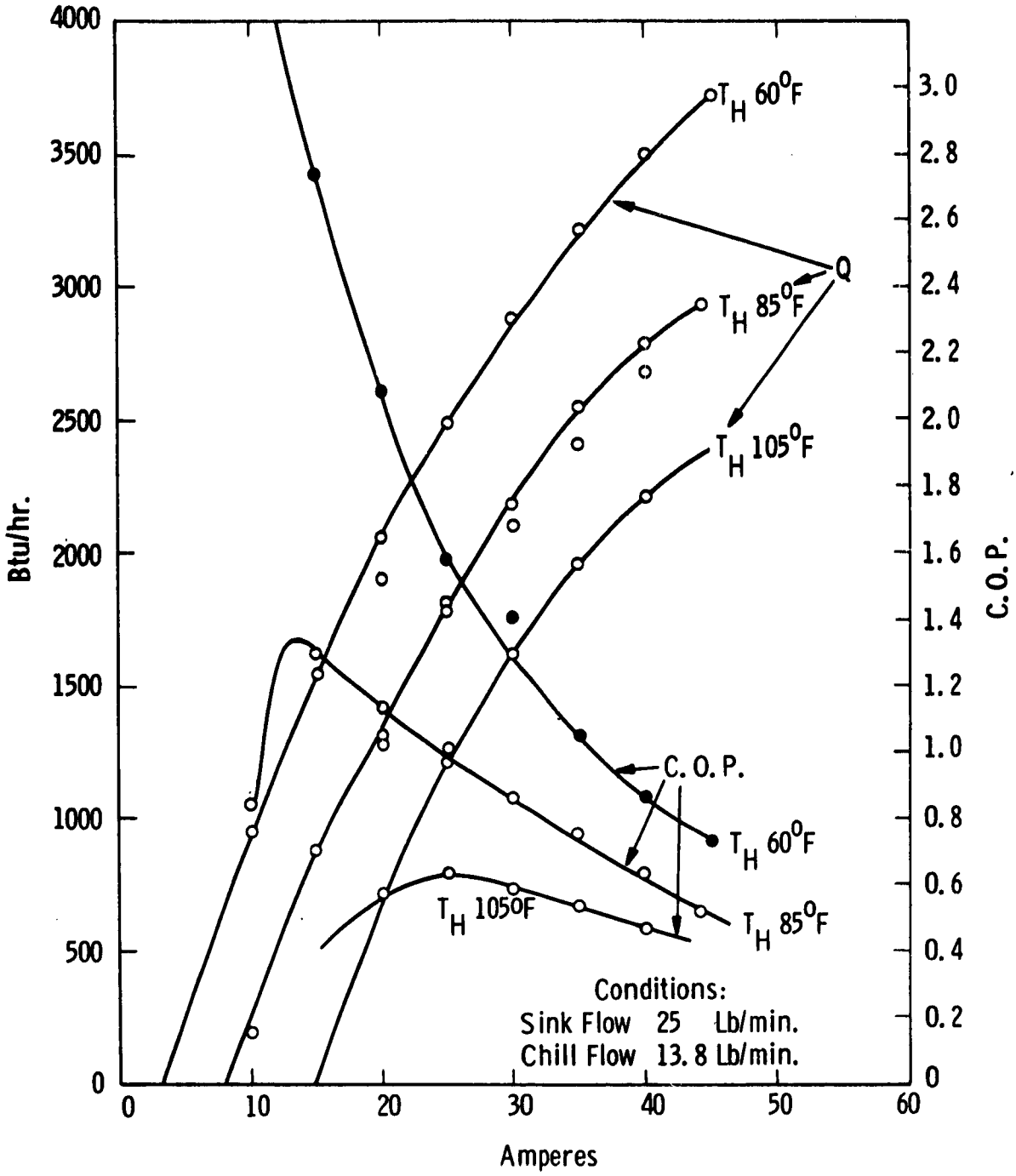

Fig. 32—Module 3 Heat Pumping Capacity vs. Current Inputs at Various Sink Water Temperatures

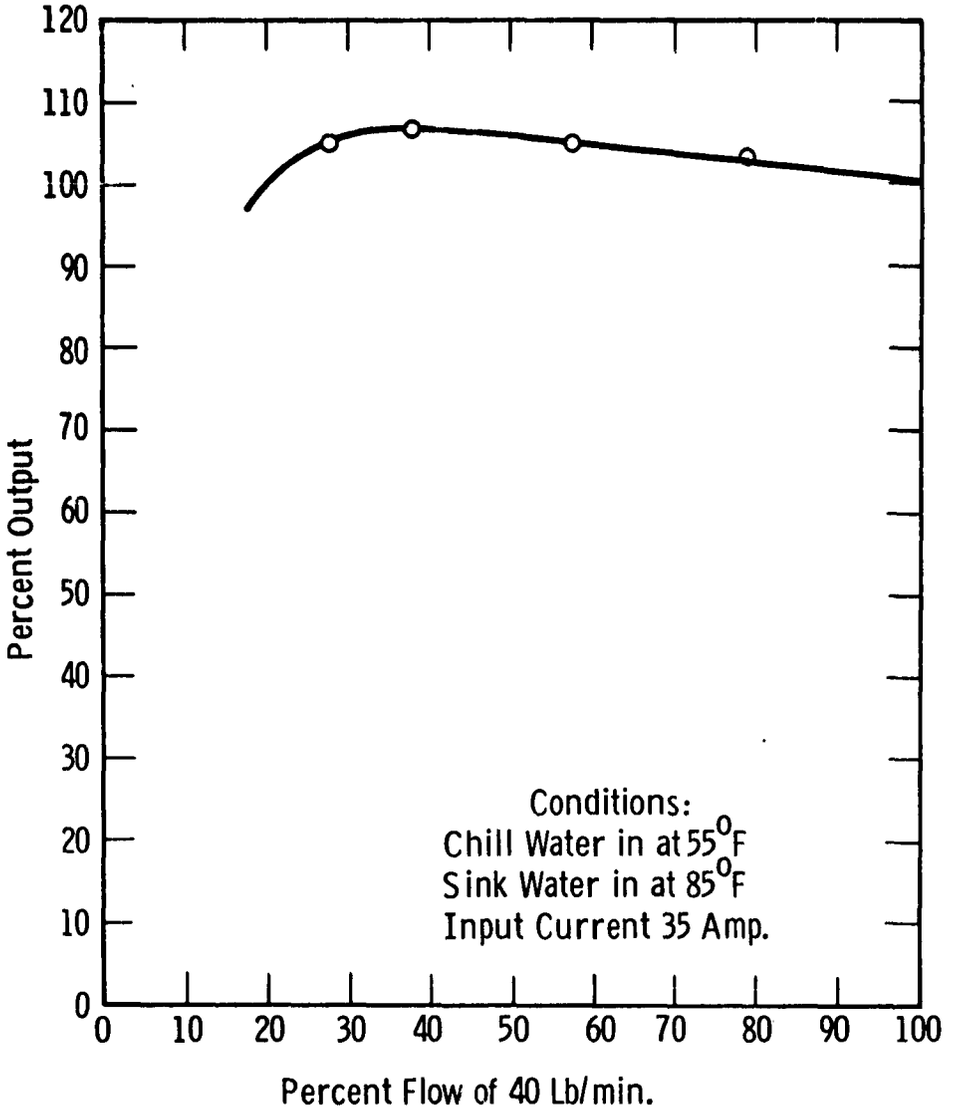

Fig. 33—Module 3 Variation of Heat Pumping Capacity vs. Chill Water Flow

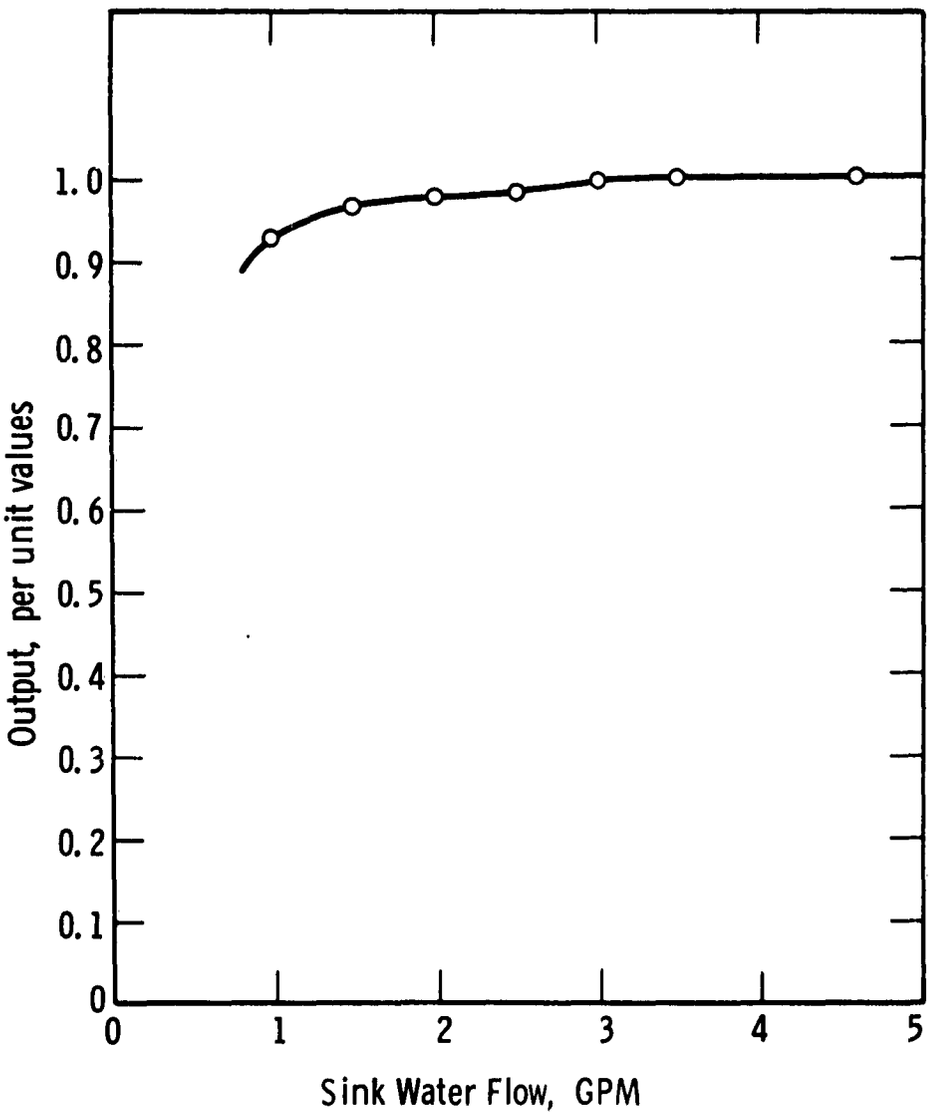

Fig. 34—Module 3 Variation of Heat Pumping Capacity vs. Sink Water Flow

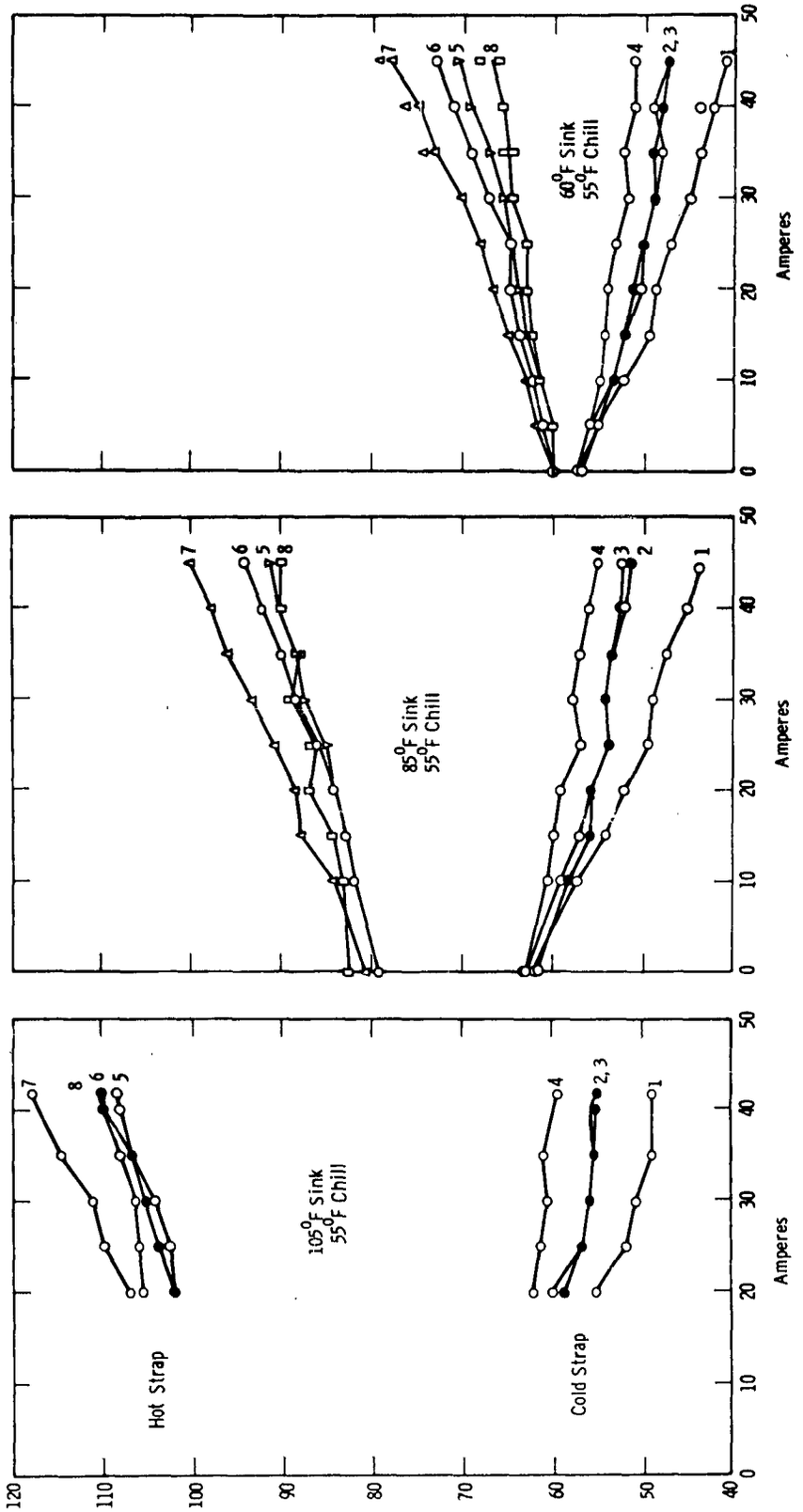

Fig. 35—Module 3 Variation of Strap Temperatures vs. Input Current

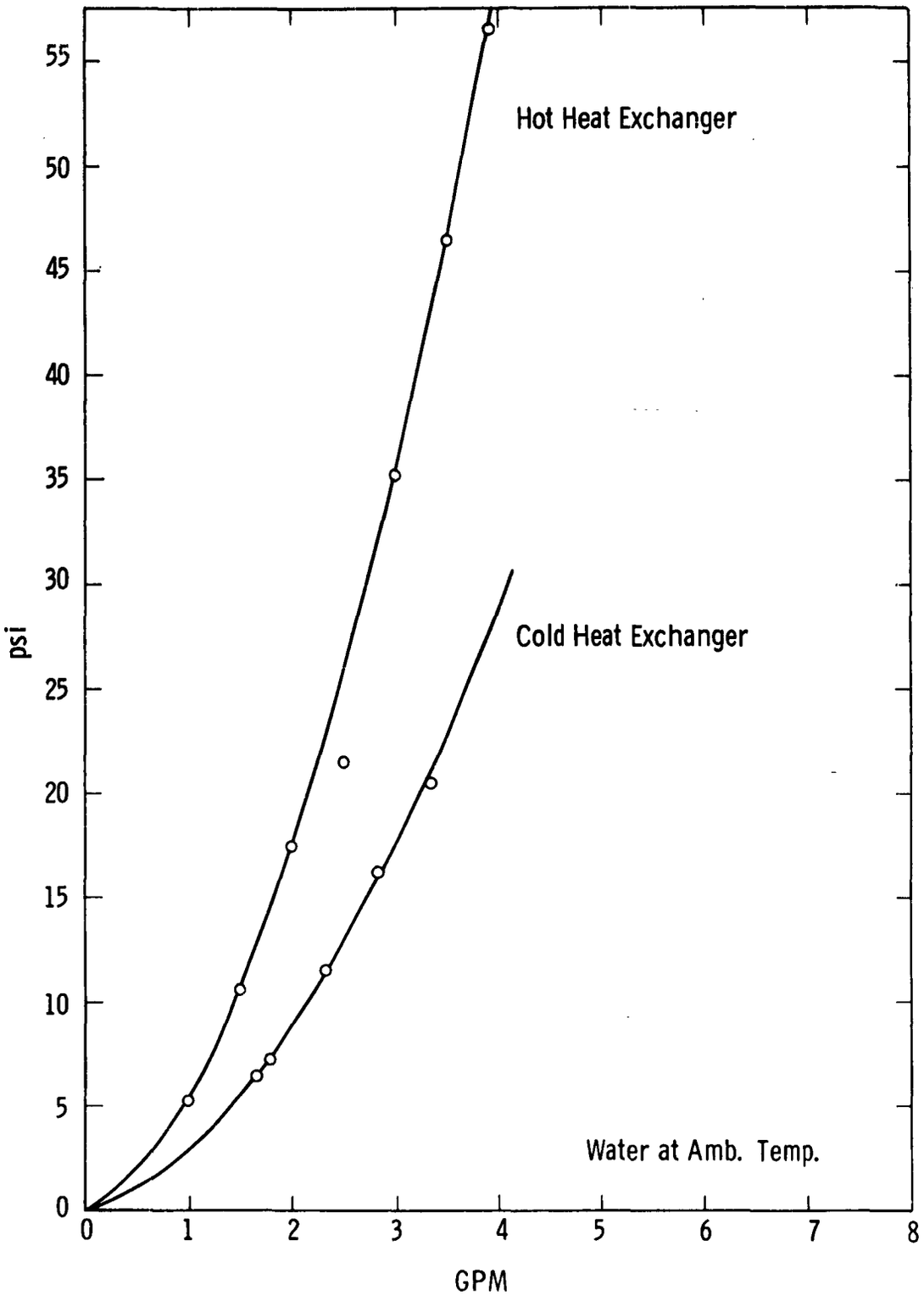

Fig. 36—Module 3 Pressure Drop vs. Water Flow Thru Heat Exchangers

During the period of this contract two other experimental units were constructed along with a 2 cubic foot freezer suitable for use in connection with a water-to-water air conditioning system. The physical characteristics of these units are shown for comparison in Table II. On the basis of the results obtained for the shipboard module at a coefficient of performance of one a ton of air conditioning could be obtained at a weight of 353 pounds and a volume of 1.76 cubic feet.

In weighing the suitability of this type of system for submarine installation the characteristics other than capacity, weight and size should be pointed out. By itself a thermoelectric unit as described here is noiseless. The only noise would come from pumps necessary to circulate the water or possibly from power supplies and controls necessary to drive the unit. This type of unit is readily assembled into different capacity units. This is a desirable feature in that it permits easier installation within cramped quarters and can also be almost exactly sized to a particular application. Ease of assembly of unit is also an important consideration for the replacement of any units which become defective. Although because of the inertness of the unit, the life should be exceptionally long. A feature of this device which is noteworthy is that sea water can be used directly in the unit. This means the sink water is at the lowest possible temperature. No additional heat exchangers with their attendant increase in temperature are needed to keep the sea water pressure from damaging the unit. This advantage is gained by using cupro-nickel tubing in the units capable of withstanding over 2000 psi.

The main disadvantage of a thermoelectric unit is of course the cost of the thermoelectric material. It should be remembered that these materials are still in the early stage of development and price reductions are certainly foreseeable. In this respect, techniques are already available whereby thinner thermoelectric materials can be made and incorporated into the module presented here. This would not only reduce the amount of material but would increase the performance of the unit.

Other than improvement in thermoelectric material there are at least three areas within which improvement can be made to gain better overall performance of the unit. The first and most important of these is the electrical insulation between the junction straps and the heat exchangers. As the heat flow must pass through this insulation it must be a good thermal conductor or so thin that the thermal loss across it can be neglected. On this unit, this insulation was provided by an aluminum oxide flame spray. Because of the porous nature of the cast aluminum heat exchangers more oxide than desired had to be sprayed on to provide the necessary electrical insulation. A pressure casting of the heat exchanger would produce a more dense material and a much thinner coat of oxide could be used. The second area concerns the weight of the unit. Approximately 30 pounds of the total 50 pounds is in the heat exchangers. Since the tubing in the heat exchangers has an outside diameter of 1/2 inch an obvious saving in weight could be made by improving the tolerance control in the casting technique so that the heat exchanger thickness could be reduced from 3/4 inch to 1/2 inch. This would represent an approximate reduction in weight of 10 pounds or 20 per cent. The final area of improvement concerns the water pressure drop through the heat exchangers. Since this pressure drop represents a loss chargeable to the performance of the unit

TABLE II PHYSICAL CHARACTERISTICS OF UNITS

UNIT	Number of Couples	Figure of Merit	T.E.Matl. Packing Density	Area occupied by T.E. Matl.	Center to center dist. of T.E.Matl.	Strap Size	Tubing Size & Matl.	Length of tubing in ea. HX	V_{OLUME}	W_{EIGHT}	Output at 85°F sink, 55°F chill and 35 amperes
MOD 1	196	2.28×10^{-3} 1/C°	18.75%	11-7/8" x 11-7/8"	0.875"	1-5/8" x 3/4" x 1/16"	0.750" O.D. 0.652" I.D. Aluminum	87"	6"x16"x 19"	78#	780BTU/HR C.O.P. 0.37
MOD 2	196	2.4×10^{-3} 1/C°	18.75%	11-7/8" x 11-7/8"	0.875"	1-5/8" x 3/4" x 1/32"	0.75" O.D. 0.652" I.D. Aluminum	105"	16-1/2"x 15" x 4-3/4"	38#	1400BTU/HR C.O.P. 0.8
MOD 3	432	2.74×10^{-3} 1/C°	49.4%	11"x11"	0.500"	$\frac{15}{16}$" x $\frac{7}{16}$" x $\frac{1}{32}$"	0.500 O.D. 0.402 I.D. 10-90 Cupro-Nickel	140"	12"x 12"x 3"	50#	2550 BTU/HR C.O.P. 0.75
FREEZER	50	2.5×10^{-3}	4.6%	14"x10-3/4"	1.500" 1.125"	cold 2-1/8x 5/8x.020 1-3/4x 5/8x.020 Hot 1-3/8x 1-9/16x.020 3-1/2x1-1/16 x .020	0.750" O.D. 0.652" I.D. Aluminum	102"	19"x 24"x 23"		

Size of Couples in All Units 0.42" Diameter x 0.25" Long
Thermal Insulation Around Thermoelectric Material was Polyurethane Foam

reduction of the loss is well worthwhile. This drop can be greatly reduced by the use of a circular coil design which has already been devised that eliminates the present 180° return bends. The pressure drop has been lowered by 90 per cent without any anticipated loss in heat exchanger performance. All these areas are related in that they represent an improvement in heat exchanger design which has been the objective throughout the project.

APPENDIX I MODULE DESIGN CALCULATIONS

Chill Water Flow Required

Under the original specifications a ton of air conditioning was to be produced with inlet and outlet water temperatures of 55°F and 50°F respectively. These requirements determined the water flow as follows:

W = lb/hr of water

h_1 = enthalpy of water at t_1 = 50°F

h_2 = enthalpy of water at t_2 = 55°F

$h_1 \approx t_1 - 32°F$

$h_2 \approx t_2 - 32°F$

Q_r = BTU/HR of cooling

$$W = \frac{Q_r}{h_2 - h_1} = \frac{Q_r}{t_2 - t_1} = \frac{12,134}{55 - 50} = 2426 \text{ lb/hr or } 4.85 \text{ gal/min.}$$

The importance of this figure changed when the construction of the module was changed so that the water flow could be connected in series or parallel in stacked units. The water flow through each module then becomes whatever is necessary or desirable. The optimum flow for the third module by tests turned out to be 13.8 pounds /minute or 1.65 gallons/minute.

Chill Water Velocity Through Heat Exchanger

Inside Diameter of Tubing = 0.404 inches

Water Flow = 13.8 pounds/minute

1.65 gallons/minute

0.22 cubic feet/minute

The velocity through the tubing would be,

$$U_m = \frac{W}{A}$$

where U_m = velocity in feet/second

W = water flow in cubic feet/second

A = cross-rectional area of tubing in square feet

$$U_m = \frac{0.22}{\pi (0.202)^2} \times \frac{144}{60} = 4.12 \text{ feet/second}$$

The Reynolds number would be,

$$N_{RE} = \frac{d\ G}{\mu}$$

where d = inside diameter of tubing in feet

G = mass velocity, $\frac{13.8 \text{ lb/min}}{\pi (0.202)^2} \times 60 \times 144 = 0.93 \times 10^6 \frac{\text{lb/hr}}{\text{ft}^2}$

μ = viscosity, 3.17 lb/hr ft @ 50°F

$$N_{RE} = \frac{0.404 \times 0.93 \times 10^6}{3.17 \times 12} \approx 1 \times 10^4$$

Temperature Drop Between Tubing and Water

The heat transfer area for 140 inches of the 0.404 inch I.D. cupro-nickel tubing in each heat exchanger is,

$$A_h = \frac{\pi\ 0.404 \times 140}{144} = 1.23 \text{ square feet}$$

The Prandtl number of water at 50°F would be,

$$N_{PR} = \frac{\mu C_p}{K} = \frac{3.17}{.334} \approx 10$$

where μ = dymanic viscosity, 3.17 lb/hr ft

C_p = heat capacity, 1 BTU/lb °F

K = thermal conductivity, 0.334 BTU/hr ft °F

The Nusselt number for a Prandtl number of 10 according to the Martinelli equation as found in "Principles of Engineering Heat Transfer" by W. H. Giedt and a Reynolds number of 10^4 would be,

$$N_{Nu} = 80$$

The heat transfer coefficient of the heat exchangers would be,

$$h = \frac{N_{Nu} K}{d} = \frac{80 \times 0.334 \times 12}{0.404}$$

$$h = 794 \text{ BTU/hour, foot}^2, \text{ °F}$$

The temperature differential from the water to the tubing for each 1000 BTU/hour of heat pumping is then,

$$\Delta T = \frac{Q}{h A_n}$$

$$\Delta T = \frac{1000}{794 \times 1.23} = 1.0°F$$

The calculations for the sink heat exchangers would differ with respect to the water temperature and flow, which were 85°F and 25 pounds/minute. The results of the calculations are listed below.

U_m = 7.45 feet/second

μ = 2.06 lb/hr ft @ 85°F

N_{RE} = 1.8×10^4

A_h = 1.23 square feet

K = 0.351 BTU/hour, foot, °F @ 85°F

N_{PR} = 5.87

$N_{NU} \approx 120$

h = 1250

ΔT = 0.8 °F per 1000 BTU/hour

Heat Loss Sink and Chill Heat Exchangers

Total Area = 12 inches x 12 inches = 144 square inches or 1 square foot

The pellet area of 432 pellets of 0.420 inch diameter and 0.25 inches long is,

$$432 \times (0.210)^2 \pi = 60 \text{ square inches}$$

The effective area is 144 minus 60 or 84 square inches. Using a thermal conductivity of 0.2 BTU/hour, inch, foot^2, °F and a maximum temperature differential of 100°F minus 45°F, the heat leakage for 1/2 the module becomes,

$$Q = \frac{K A}{L} \Delta T = \frac{0.2 \times 1 \times 55}{0.25} = 44 \text{ BTU/hour}$$

For the whole module the leakage is twice this or 88 BTU/hour.

The heat pumping ability of a thermoelectric pellet is calculated by solving the heat pumping equation:

$$Q = \pi I - 1/2\ R\ I^2 - \frac{K\ A}{L}(T_h - T_c)$$

where π = average Peltier coefficient for a couple

I = D.C. current plus a ripple factor

R = one half total couple resistance

K = average thermal conductivity of the thermoelectric couple

A = cross-sectional area of a pellet

L = length of a pellet

T_h = hot junction temperature

T_c = cold junction temperature

Solving of the equation in this manner one can obtain a family of curves of heat pumping versus input current at various hot junction temperature and a specific cold junction temperature. This computation is easily done on a computor. An example of the curves obtainable is shown in Figures 37 and 38. The coefficient of performance is obtained by the equation,

$$C.O.P. = \frac{Q}{(IR + \pi)I}$$

where Q = heat pumping rate

I = D.C. input current

π = Peltier coefficient

R = total circuit resistance

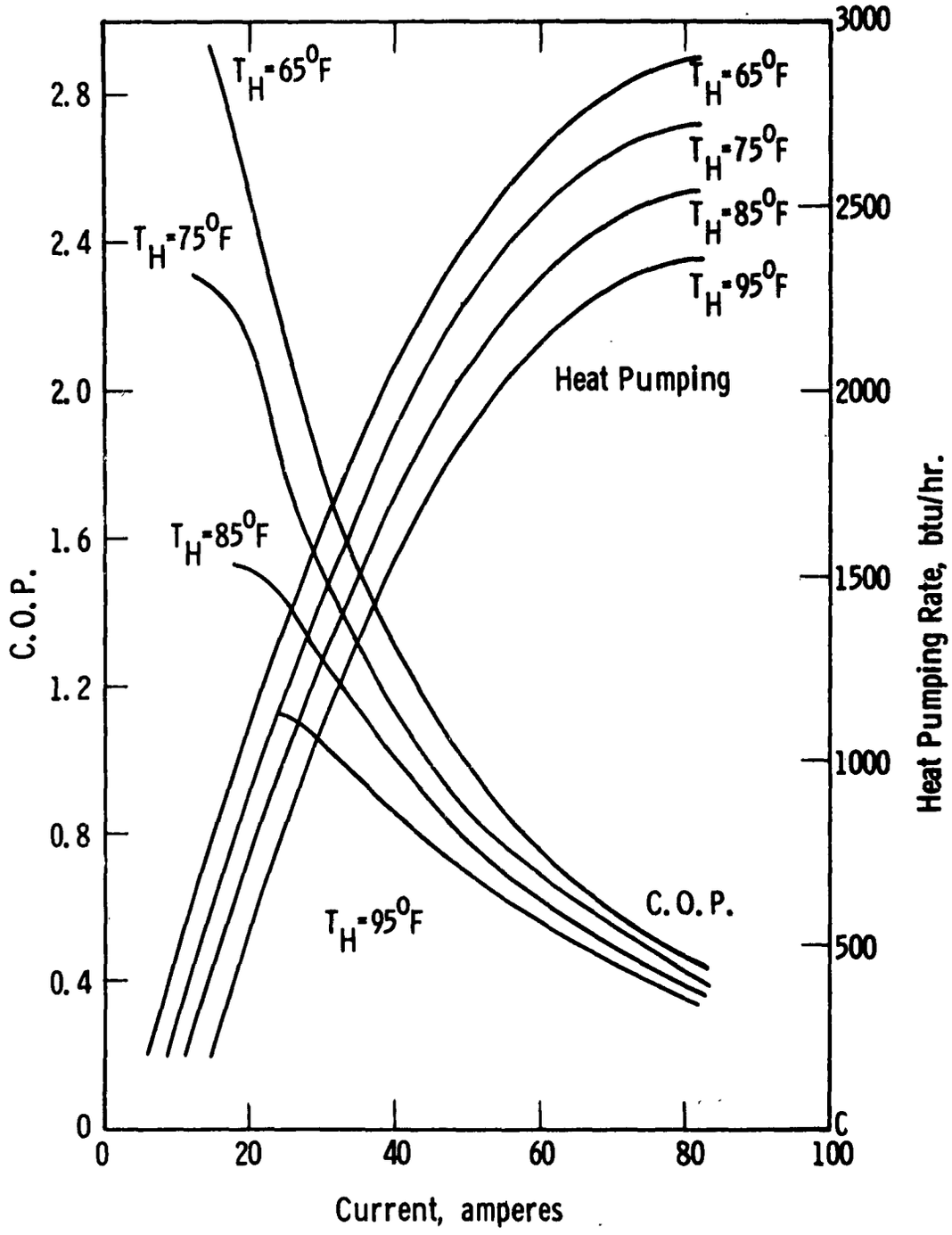

Fig. 37—Module 3 Calculated Performance with Z of 2.6 for 1/2 Module

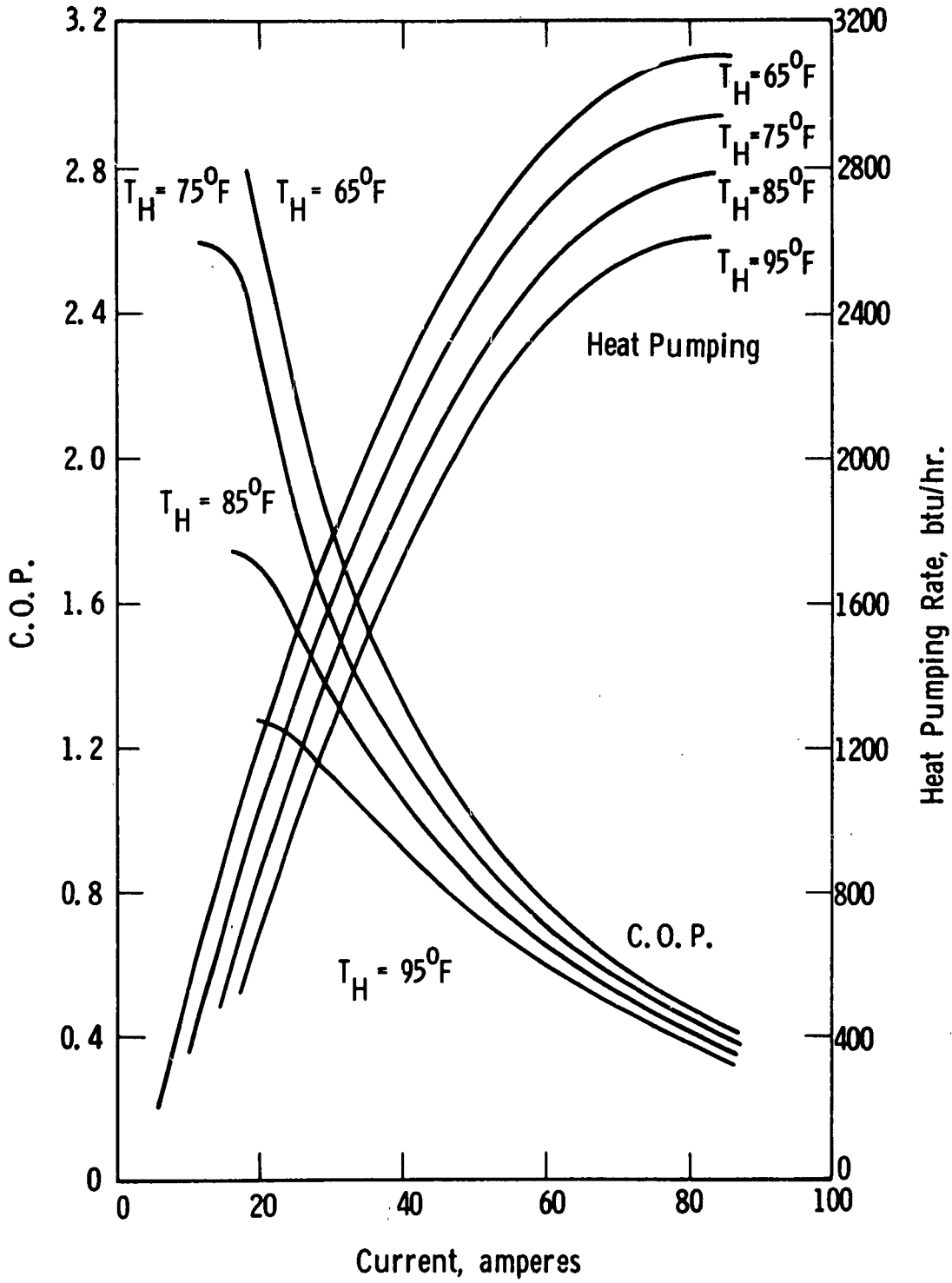

Fig. 38—Module 3 Calculated Performance with Z of 2.95 for 1/2 Module

The curves obtained in this manner are independent of the heat exchangers used on the hot and cold junctions. How closely the performance of a completed unit would follow these curves depends on the ability of the heat exchangers to remove the heat without additional temperature drop. A perfect heat exchanger would be one in which the water was at the same temperature as the thermoelectric junctions.

APPENDIX II FREEZER DESIGN CALCULATIONS

Heat Leakage Into Box

The various inside areas of the freezer were first determined.

L1 - Top and bottom 16 x 17 1/2 x 2 = 560 sq in or 3.9 sq ft

L2 - Sides 13 1/2 x 17 1/2 x 2 = 472 sq in or 3.3 sq ft

L3 - Door 13 1/2 x 16 = 216 sq in or 1.5 sq ft

L4 - Thermoelectric unit 13 1/2 x 16 = 216 sq in or 1.5 sq ft

The polyurethane foam used for insulation was 4 inches thick in the top, bottom, and sides, 3 inches thick in the door, and 3/4 inch thick between the hot and cold plates of the thermoelectric assembly. A value of 0.2 BTU/hr., inch, ft^2, ^oF was used for its thermal conductivity. A maximum ambient of 85^oF was considered outside the freezer and an internal air temperature of -10^oF. Using the basic equation for heat flow by conduction,

$$Q = K \frac{A}{L} \Delta T$$

the various leakage were determined.

$$Q_{L1} = \frac{0.2 \times 3.9 \times 95}{4} = 18.5 \text{ BTU/hr}$$

$$Q_{L2} = \frac{0.2 \times 3.3 \times 95}{4} = 15.7 \text{ BTU/hr}$$

$$Q_{L3} = \frac{0.2 \times 1.5 \times 95}{4} = 9.5 \text{ BTU/hr}$$

To obtain the heat leakage of the thermoelectric unit the area occupied by the pellets must be subtracted from the total area to obtain the effective area. 100 pellets with diameter of 0.420 inches and 0.25 length were used in the assembly. The pellet cross-sectional area was,

$$100 \times \pi (0.210)^2 = 13.9 \text{ square inches or } 0.1 \text{ square feet}$$

As the sink water used in the thermoelectric unit will be between 50° - 60°F the temperature differential between the hot and cold plates will be from 60°F to -10°F or 70°F. Therefore,

$$Q_{LA} = \frac{0.2 (1.5 - .1) 70}{0.75} = 26.2 \text{ BTU/hr}$$

The total heat leakage into the freezer box would be,

$$Q_{LT} = 18.5 + 15.7 + 9.5 + 26.2 = 70 \text{ BTU/hr}$$

This would be the steady state load on the thermoelectric unit in an ambient of 85°F.

Cold Side Heat Exchanger

The heat was transferred inside the freezer to the thermoelectric junctions by means of a finned natural convection heat exchanger. It was composed of 30 alumimum fins, 0.032 inches thick, 12 inches thick, and 1.5 inches long. The spacing between fins was 0.5 inches. The heat load to be exchanged was the total pumping load less the leakage through the thermoelectric unit or 43.8 BTU/hour.

$$\text{Fin area} = \frac{1.5 \times 12 \times 30 \times 2}{144} = 7.5 \text{ square feet}$$

The fin efficiency was determined by the equation,

$$\eta_F = \frac{\tanh m\ell}{m\ell}$$

where $m = \sqrt{\frac{2h}{tK}}$

ℓ = length of fin in feet

h = heat transfer coefficient

t = thickness of fin in feet

K = thermal conductivity of fin, 170 BTU/hour, foot $^{\circ}F$

For this type of finned heat exchanger the convective heat transfer coefficient is approximately,

$$h \approx 1.0 \text{ BTU/hour, ft}^2\ ^{\circ}F$$

Continuing with the determination of the fin efficiency,

$$m = \sqrt{\frac{2 \times 1 \times 12}{0.032 \times 170}} = 2.1$$

$$\eta_F = \frac{\tanh 2.1 \times 1.5/12}{2.1 \times 1.5/12} = \frac{\tanh 0.26}{0.26} \approx 100\%$$

The temperature difference between the fins and the air inside the freezer would be,

$$\Delta T = \frac{Q}{h A \eta_F} = \frac{43.8}{1 \times 7.5 \times 1} = 5.8^{\circ}F$$

Hot Side Heat Exchanger

This heat exchanger consisted of 102 inches of 0.65 inch I. D. aluminum tubing brazed to a flat aluminum plate. The heat transfer area of this tubing would be,

$$A = \frac{\pi \times 0.65 \times 102}{12} = 1.74 \text{ square feet}$$

A water flow of 2426 pounds/hour at 50°F was assumed through the tubing. The mass velocity was then,

$$G = \frac{2426}{\pi (0.325)^2} = 1.05 \times 10^6 \text{ pounds/hour, square feet}$$

The viscosity μ, of water at 50°F being 3.17 pounds, hour, foot. The Reynolds number in the coiled tubing was,

$$N_{RE} = \frac{d\ G}{\mu} = \frac{0.65 \times 1.05 \times 10^6}{3.17 \times 12} = 1.8 \times 10^4$$

The Prandtl number of water at 50°F would be,

$$N_{PR} = \frac{\mu\ C_p}{K} = \frac{3.17}{.334} \approx 10$$

where μ = dynamic viscosity, lb/hr ft

C_p = heat capacity, BTU/lb °F

K = thermal conductivity, BTU/hr ft °F

The Nusselt number for a Prandtl number of 10 according to the Martinelli equation as found in "Principles of Engineering Heat Transfer" by W. H. Giedt and a Reynolds number of 1.8×10^4 would be,

$$N_{NU} = 100$$

The heat transfer coefficient then becomes

$$h = \frac{N_{NU}\ K}{d} = \frac{100 \times 0.334 \times 12}{0.65}$$

$$h = 616 \text{ BTU/hour, square foot, } ^\circ F$$

From Figure 39 which is a plot of the heat pumping rates versus coefficient of performance for various figures of merit it can be seen that the curve for a figure of merit of 2.59×10^{-3} $1/C^{\circ}$ is leveling off at a coefficient of performance slightly over 0.3. Using this value the total heat to be dissipated in the sink water would be,

$$\frac{Q_{LT}}{0.3} + Q_{LT} = \frac{70}{0.3} + 70 = 230 + 70 = 300 \text{ BTU/hour}$$

The temperature difference between the sink water and the hot heat exchanger would be,

$$\Delta T = \frac{Q}{h A} = \frac{300}{616 \times 1.74} = 0.28^{\circ}F$$

Time Required to Reach Operating Temperature

Assuming an initial temperature of $90^{\circ}F$ and a desired final temperature of $0^{\circ}F$ the total heat removal necessary was determined.

1. Air within Freezer

   Volume = 2.1 cubic feet
   Density = 0.072 pounds/ cubic foot
   Specific Heat = 0.24 BTU/pound$^{\circ}F$

   $q = V_{\rho} C_{\rho} \Delta T = 2.1 \times 0.072 \times 0.24 (90^{\circ} - 0^{\circ})$

   $q = 3.26$ BTU

2. Cold Plate and Fins

   Volume = 0.0342 cubic feet
   Density = 170 pounds/cubic foot
   Specific Heat = 0.22 BTU/pound$^{\circ}F$

   $q = V_{\rho} C_{\rho} \Delta T = 0.0342 \times 170 \times 0.22 (90^{\circ} + 10^{\circ})$

   $q = 128$ BTU

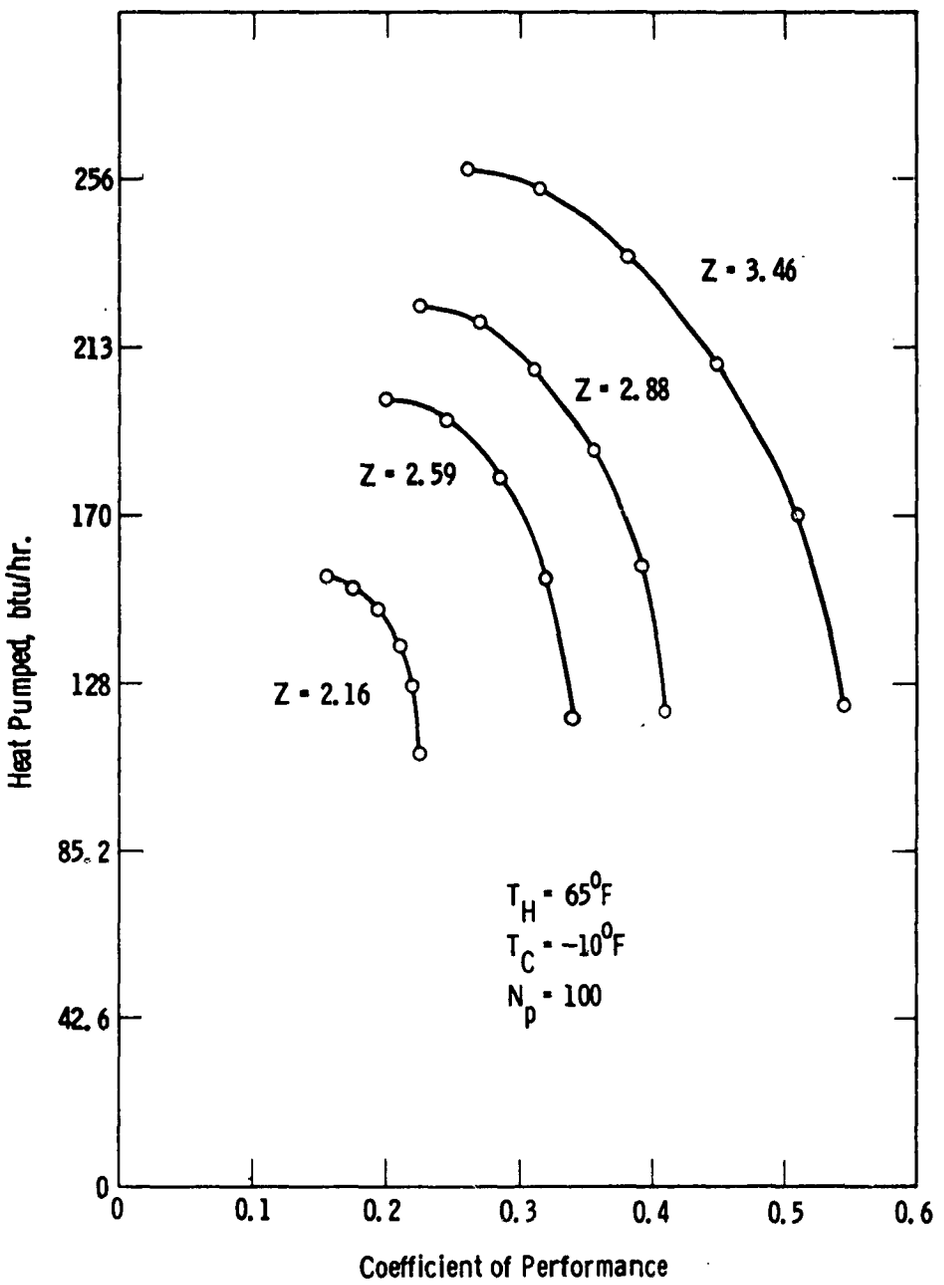

Fig. 39—Freezer Heat Pumping vs. C.O.P. for Various Figure of Merits

3. Freezer Insulation

Volume = 2.6 cubic inches
Denisty = 5.3 pounds/cubic foot
Specific Heat = 0.2 BTU/pound ^{o}F

$$q = V_{\rho}\, C_{\rho}\, \Delta T = 2.6 \times 5.3 \times 0.2 \left(\frac{90^{o} - 0^{o}}{2}\right)$$

$$q = 124 \text{ BTU}$$

4. Total Heat to be Removed in One Hour

$$Q_{T} = 3 + 128 + 124 = 255 \text{ BTU}$$

In Figure 40 is a plot of the heat pumping rates versus input currents at various cold junction temperatures for a figure of merit of 2.59×10^{-3} 1/C^{o}. Since the cold junction will almost immediately reach the hot junction temperature when the sink water is turned on, it is assumed the heat pumping will start with a cold junction temperature of 50^{o}F. Using a current of 35 amperes the heat pumping rate would start at 450 BTU/hour and decline to 150 BTU/hour at -10^{o}F. This would be an average pumping rate of 300 BTU/hour.

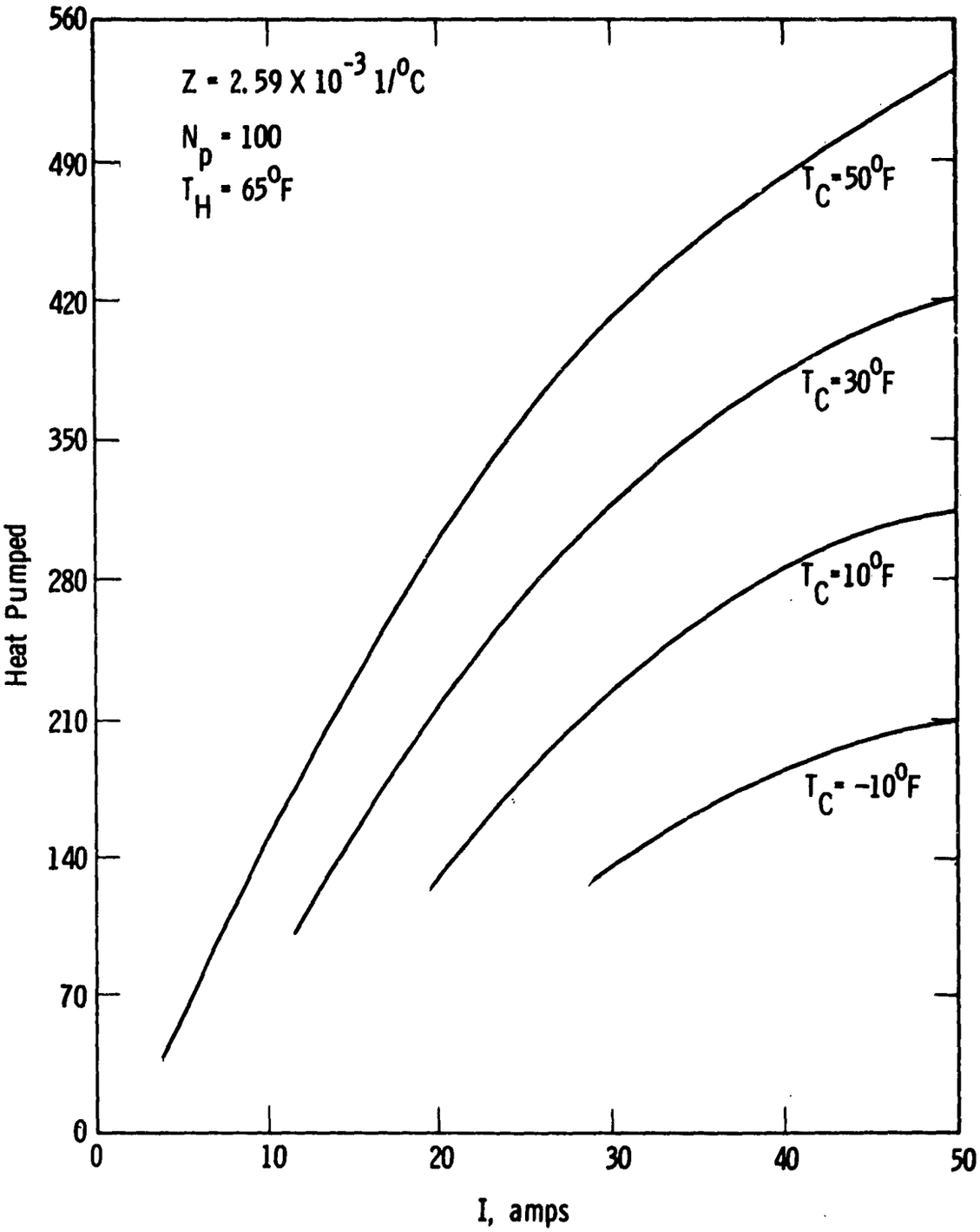

Fig. 40—Freezer Heat Pumped vs. Input Current

APPENDIX III - SHOCK TESTS

9700-916CPTFR

FACTORY TEST RECORD
CLASS III SHOCK
NAVEXOS- 3373

Issued by the Navy Department, Washington, D. C.
To be used in connection with Military Specification MIL-S-901. -B Paragraph 4.4.1.1

DATE: April 11, 1961

TEST NO.: 721133

1. ITEM NAME OF EQUIPMENT SHOCK-TESTED: Navy Submarine Air Conditioning Module

2. RATING (KW, VOLTS, RPM, CPM, ETC.): Input 220 V 3 Phase 60 cyc, Output 35 A. 24 1/2 V.

3. MAJOR PARTS

	MANUFACTURER	ADDRESS	IDENTIFYING NUMBER
PUMP, ETC.	Supplier Westinghouse Electric Corp. at	Cheswick, Pa.	
MOTOR, ETC.			
STARTER, ETC.			
Tested by W. C. Gregson at Westinghouse Electric Corp.		East Pittsburgh, Pa.	

4. DATA REGARDING THE CONTRACTOR — CONTRACTOR: — CONTRACT NUMBER: Nobs 77095

5. TYPE OF SHOCK TEST (INDICATE): ☐ COMPLETE ASSEMBLY ☐ SUB-ASSEMBLY ☐ PART

6. TOTAL WEIGHT OF ASSEMBLY TESTED: _____ LBS. — WEIGHT OF INDIVIDUAL MAJOR PARTS (COMPRESSOR, ETC.): _____ LBS. — MOTOR (ETC.): _____ LBS. — STARTER (ETC.): _____ LBS.

7. WEIGHT CLASSIFIED OF ITEM (INDICATE): ☒ LIGHT ☐ MEDIUM

8. APPLICABLE MOUNTING FIGURE IN SPECIFICATION MIL-S-901 (INDICATE): ☐ 4A ☒ 4C ☐ 6D ☐ 6E ☐ 7A ☐ OTHER (SPECIFY)

Photo 370117

9. FOR LIGHTWEIGHT ITEMS

FIRST CONDITION				SECOND CONDITION			
BLOW NO.	DROP IN FEET	AXIS	DAMAGE INCURRED	BLOW NO.	DROP IN FEET	AXIS	DAMAGE INCURRED
1	1	FIRST AXIS (BACK) Top	OK	1	1	FIRST AXIS (BACK)	
2	3	FIRST AXIS (BACK) Top	OK	2	3	FIRST AXIS (BACK)	
3	5	FIRST AXIS (BACK) Top	OK	3	5	FIRST AXIS (BACK)	Witnesses:
4	1	SECOND AXIS (SIDE) Back	OK	4	1	SECOND AXIS (SIDE)	Ed Frantti Cheswick
5	3	SECOND AXIS (SIDE) Back	OK	5	3	SECOND AXIS (SIDE)	Jim Duch Cheswick
6	5	SECOND AXIS (SIDE) Back	OK	6	5	SECOND AXIS (SIDE)	
7	1	THIRD AXIS (TOP) Side	OK	7	1	THIRD AXIS (TOP)	
8	3	THIRD AXIS (TOP) Side	OK	8	3	THIRD AXIS (TOP)	
9	5	THIRD AXIS (TOP) Side	OK	9	5	THIRD AXIS (TOP)	

WHETHER SAME OR DIFFERENT ITEMS WERE SUBJECTED TO ABOVE TWO CONDITIONS

REMARKS: Test witnessed by D. E. Burg 8-31-61 Navy Inspector
Post shock test examination to be at point of manufacture

10. FOR MEDIUM-WEIGHT ITEMS (Hammer Drop)

BLOW NO.	GROUP NO.	HAMMER DROP IN FEET	DAMAGE INCURRED	BLOW NO.	GROUP NO.	HAMMER DROP IN FEET	DAMAGE INCURRED
1	I			4	II		
2	I			5	III		
3	II			6	III		

TOTAL WEIGHT ON ANVIL TABLE: _____ LBS.

REMARKS

68

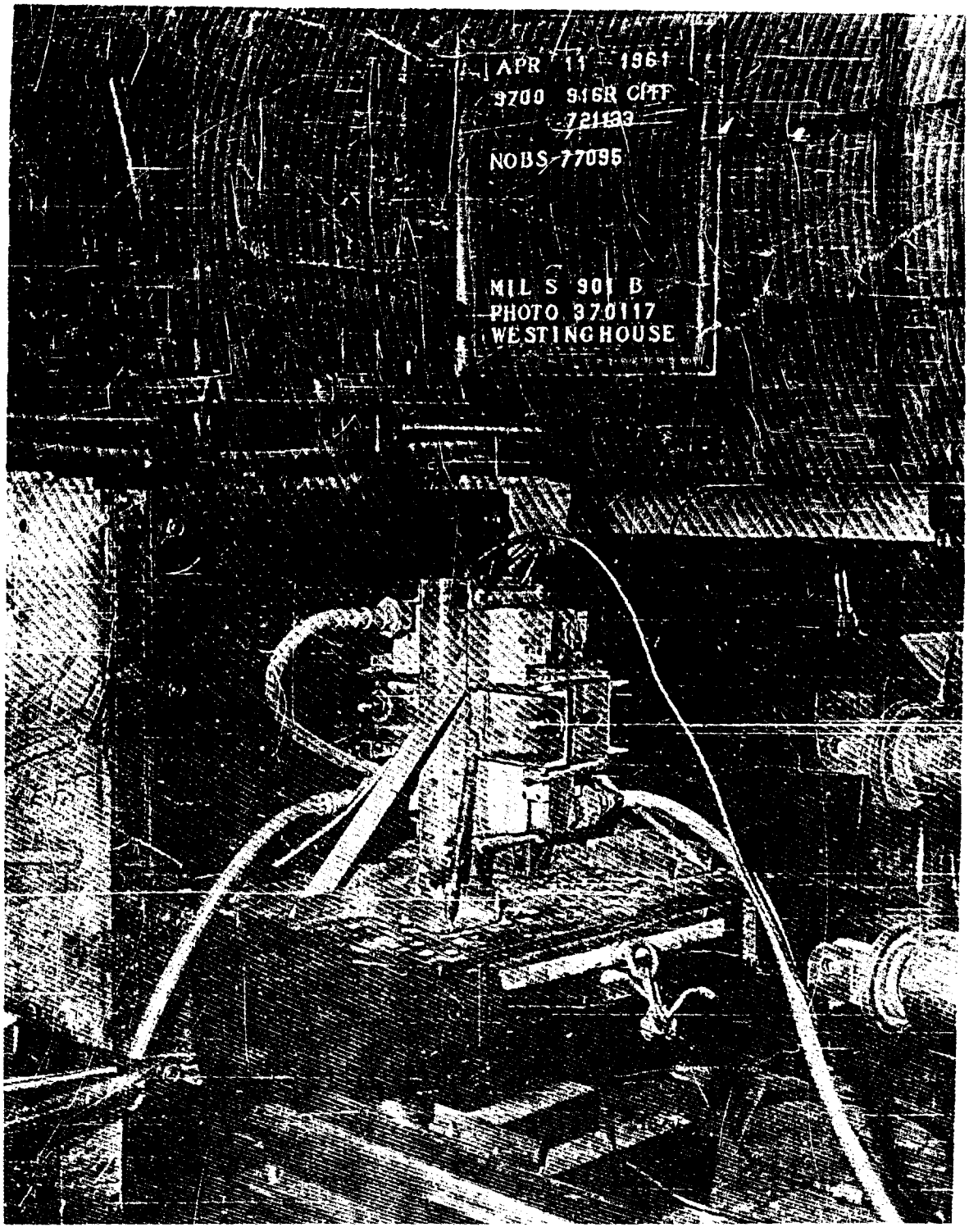

Figure 41 First Shock Test Setup

9700-916CFFFR

FACTORY TEST RECORD
CLASS BI SHOCK
MAYERS-5573

Issued by the Navy Department, Washington, D. C.
To be used in connection with Military Specification MIL-S-901 -B Paragraph 4.4.1.1

DATE: April 21, 1961

TEST NO.: 721133

1. ITEM NAME OF EQUIPMENT SHOCK-TESTED: Navy Submarine Air Conditioning Module

2. RATING (KW, VOLTS, RPM, CPM, ETC.): Input 220 V 3 Phase 60 cyc, Output 35 A. 29 V.

3. MAJOR PARTS

	MANUFACTURER	ADDRESS	IDENTIFYING NUMBER
PUMP, ETC.	Supplier Westinghouse Electric Corp.	at Cheswick,Pa.	
MOTOR, ETC.			
STARTER, ETC.			
	Tested by W. C. Gregson at Westinghouse Electric Corp.	East Pittsburgh, Pa.	

4. DATA REGARDING THE CONTRACTOR — CONTRACTOR: Water cold 48°F Warm 84.7°F — CONTRACT NUMBER: Nobs 77095

5. TYPE OF SHOCK TEST (INDICATE): ☐ COMPLETE ASSEMBLY ☐ SUB-ASSEMBLY ☐ PART

6. TOTAL WEIGHT OF ASSEMBLY TESTED: _____ LBS. — WEIGHT OF INDIVIDUAL MAJOR PARTS (COMPRESSOR, ETC.): _____ LBS. — MOTOR (ETC.): _____ LBS. — STARTER (ETC.): _____ LBS.

7. WEIGHT CLASSIFIED OF ITEM (INDICATE): [X] LIGHT ☐ MEDIUM

8. APPLICABLE MOUNTING FIGURE IN SPECIFICATION MIL-S-901 (INDICATE): ☐ 4A [X] 4C ☐ 6D ☐ 6E ☐ 7A ☐ OTHER (SPECIFY)

Photo 370123

9. FOR LIGHTWEIGHT ITEMS

FIRST CONDITION				SECOND CONDITION			
BLOW NO.	DROP IN FEET	AXIS	DAMAGE INCURRED	BLOW NO.	DROP IN FEET	AXIS	DAMAGE INCURRED
1	1	FIRST AXIS (BACK) Top	OK	1	1	FIRST AXIS (BACK)	
2	3	FIRST AXIS (BACK) Top	OK	2	3	FIRST AXIS (BACK)	
3	5	FIRST AXIS (BACK) Top	OK	3	5	FIRST AXIS (BACK)	Witnesses;
4	1	SECOND AXIS (SIDE) Back	OK	4	1	SECOND AXIS (SIDE)	Ed Frantti Cheswick
5	3	SECOND AXIS (SIDE) Back	OK	5	3	SECOND AXIS (SIDE)	Jim Duch Cheswick
6	5	SECOND AXIS (SIDE) Back	OK	6	5	SECOND AXIS (SIDE)	
7	1	THIRD AXIS (TOP) Side	OK	7	1	THIRD AXIS (TOP)	
8	3	THIRD AXIS (TOP) Side	OK	8	3	THIRD AXIS (TOP)	
9	5	THIRD AXIS (TOP) Side	Water Warm 91.3°F OK	9	5	THIRD AXIS (TOP)	

WHETHER SAME OR DIFFERENT ITEMS WERE SUBJECTED TO ABOVE TWO CONDITIONS

REMARKS: Test witnessed by A. Seech Al Seech, Navy Inspector
Post shock test examination to be at point of Manufacture

10. FOR MEDIUM-WEIGHT ITEMS (Hammer Drop)

BLOW NO.	GROUP NO.	HAMMER DROP IN FEET	DAMAGE INCURRED	BLOW NO.	GROUP NO.	HAMMER DROP IN FEET	DAMAGE INCURRED
1	I			4	II		
2	I			5	III		
3	II			6	III		

TOTAL WEIGHT ON ANVIL TABLE: _____ LBS.

REMARKS

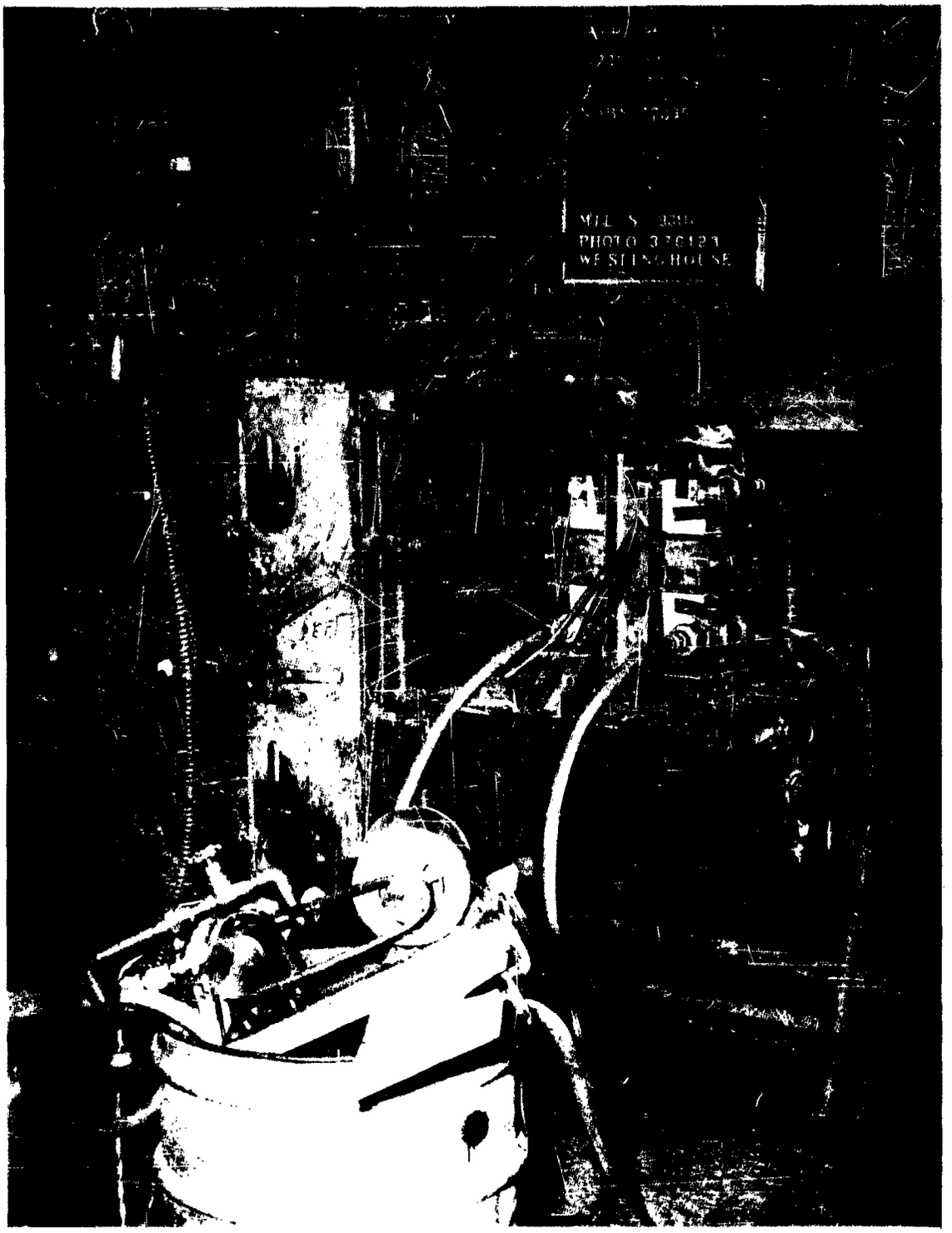

Figure 42 Second Shock Test Setup

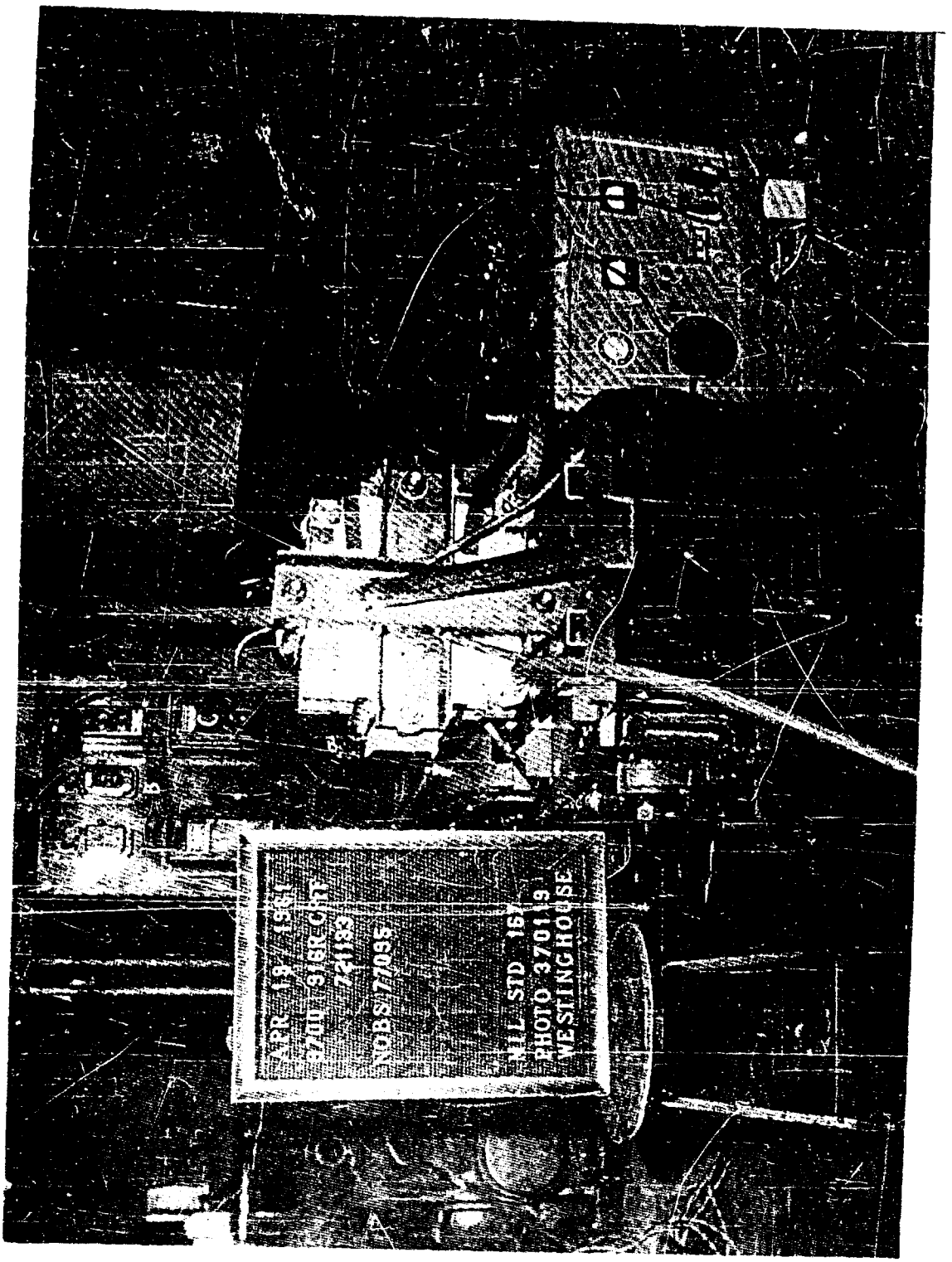

Figure 43 Vibration Test Fore & Aft Position

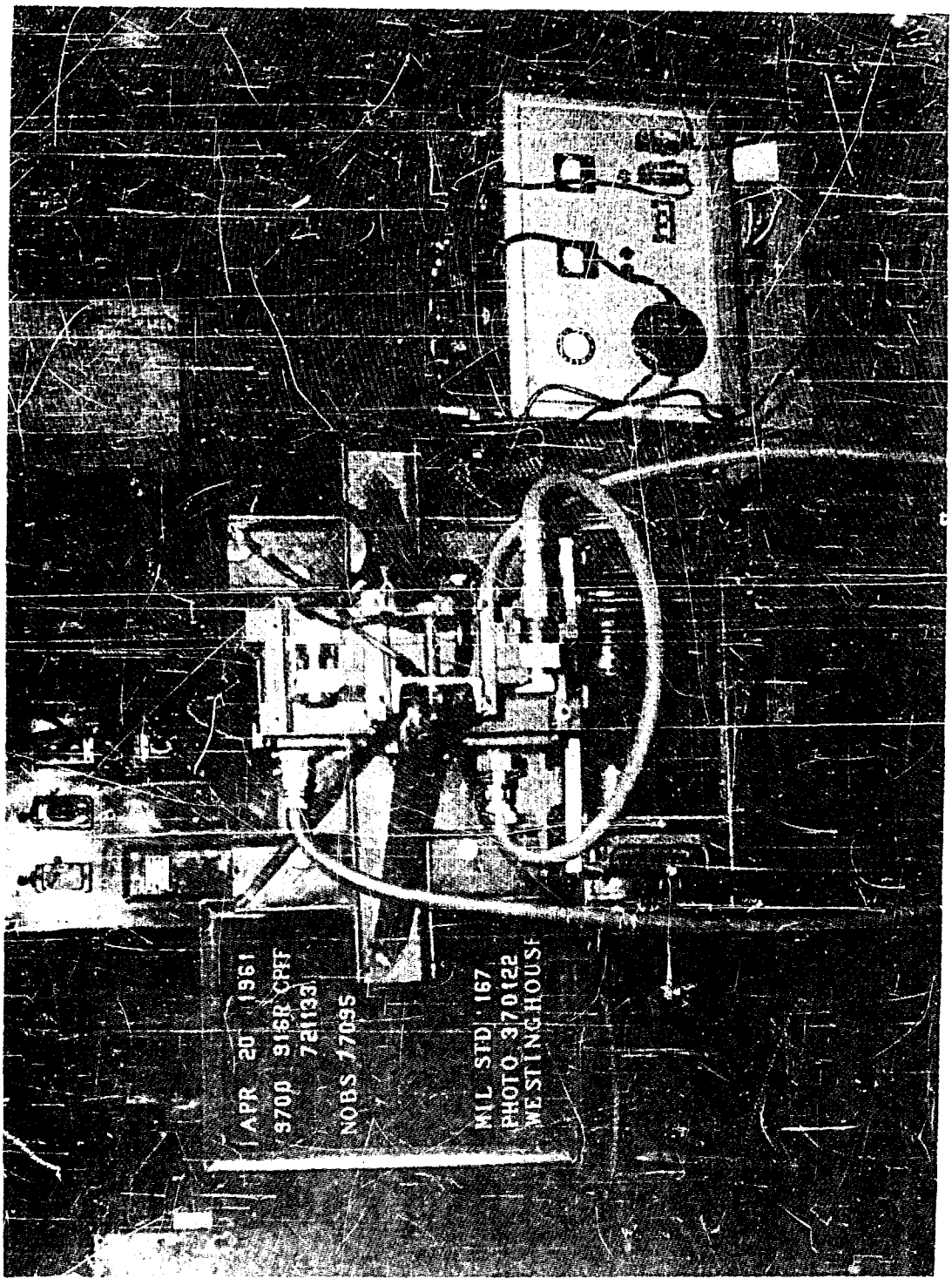

Figure 44 Vibration Test Vertical Position

APPENDIX IV VIBRATION TESTS

Navy Submarine Air Conditioning Module
I.W.R. 9700-916-R-721133
Vibration Tests as per MIL-STD-167
Nobs 77095
Unit energized with 35 Amps. and 26 volts
Photo #370119

Fore and Aft

Exploratory Vibration (Par.3.1.4.3.1)
9 C.P.S. to 33 C.P.S. .010 in. Amplitude No Resonant Points

Variable Frequency Test (Par. 3.1.4.3.2) (5 min. at each point)
9 C.P.S. to 15 C.P.S. .030 in. Amplitude
16 C.P.S. to 25 C.P.S. .020 in. Amplitude
26 C.P.S. to 33 C.P.S. .010 in. Amplitude

Endurance Test (Par. 3.1.4.3.3) 2 Hours
33 C.P.S. .010 Amplitude

Athwart Ships

Repeated Tests of Par. 3.1.4.3.1, 3.1.4.3.2 and 3.1.4.3.3.

Vertical

The vertical position was simulated by mounting unit 90° to Vibration Table. (See Photo #370122).

Exploratory Vibration (Par. 3.1.4.3.1)
9 C.P.S. to 33 C.P.S. .010 in. Amplitude Resonance at 31 C.P.S.

Variable Frequency (Par. 3.1.4.3.2) (5 min. at each point)
9 C.P.S. to 15 C.P.S. .030 in. Amplitude
16 C.P.S. to 25 C.P.S. .020 in. Amplitude
26 C.P.S. to 33 C.P.S. .010 in. Amplitude

Endurance Test (Par. 3.1.4.3.3) 2 Hours
29 C.P.S. .010 Amplitude

These test Results Observed by J. Berg, Navy Inspection Dept. Also witnessed by E. Frantti and J. Duch, New Products, Central Laboratories.

Tested by Walter Payne, 2-LRwy Lab., East Pittsburgh, Pa.

DISTRIBUTION LIST

Mr. M. J. Pistilli, Office of Inspector of Naval Material, 401 Old Post Office Building, Pittsburgh 19, Pennsylvania.

Mr. R. T. Fiske, Marine Department, Westinghouse Washington Office (3)

Mr. B. J. Wilson (Code 5230), Director, U. S. Naval Research Lab., Washington.

Lt. Cdr. J. Woolston (Code 241E), Commander, Portsmouth Naval Shipyard, Portsmouth, New Hampshire.

Mr. R. J. Kirkpatrick, Headquarters Engineering Staff, Research Labs, Pittsburgh, Pennsylvania.

Mr. W. G. Evans, Project Manager, New Products Laboratories, Churchill Boro, Pgh. 35, Pa.

Mr. J. D. Meess, Supervising Engineer, New Products Laboratories, Churchill Boro, Pgh. 35, Pa.

Mr. G. W. Nagel, Advisory Engineer, New Products Laboratories, Churchill Boro, Pgh. 35, Pa.